Neurotherapeutics

Behavioral and cognitive improvement induced by novel imidazoline I2 receptor ligands in female SAMP8 mice

--Manuscript Draft--

Manuscript Number:	NERX-D-18-00153R4
Full Title:	Behavioral and cognitive improvement induced by novel imidazoline I2 receptor ligands in female SAMP8 mice
Article Type:	Original Article
Corresponding Author:	Mercè Pallàs, PhD SPAIN
Corresponding Author Secondary Information:	
Corresponding Author's Institution:	
Corresponding Author's Secondary Institution:	
First Author:	Christian Griñán-Ferré
First Author Secondary Information:	
Order of Authors:	Christian Griñán-Ferré
	Foteini Vasilopoulou
	Sonia Abàs
	Sergio Rodriguez-Arevalo
	Andrea Bagan
	Francesc X Sureda
	Belen Pérez
	Luis F Callado
	Jesús A García-Sevilla
	M. Julia García- Fuster
	Carmen Escolano
	Mercè Pallàs, PhD
Order of Authors Secondary Information:	
Funding Information:	Ministerio de Economía y Competitividad of Spain (SAF2016-33307) — Dr. Mercè Pallàs
	Ministerio de Economía y Competitividad of Spain (SAF2014-55903-R) — Dr M. Julia García- Fuster
	Basque Government (IT616/13) — Dr Luis F Callado
	Association Belge contre les Maladies Neuro-Musculaires (BE) (2017SGR106) — Dr. Mercè Pallàs
Abstract:	As populations increase their life expectancy, age-related neurodegenerative disorders such as Alzheimer's disease have become more common. I2-Imidazoline receptors (I2-IR) are widely distributed in the central nervous system, and dysregulation of I2-IR in patients with neurodegenerative diseases has been reported, suggesting their implication in cognitive impairment. This evidence indicates that high-affinity selective I2-IR ligands potentially contribute to the delay of neurodegeneration. In vivo studies in

	the female senescence accelerated mouse-prone 8 mice have shown that treatment with I2-IR ligands, MCR5 and MCR9, produce beneficial effects in behavior and cognition. Changes in molecular pathways implicated in oxidative stress, inflammation, synaptic plasticity, and apoptotic cell death were also studied. Furthermore, treatments with these I2-IR ligands diminished the amyloid precursor protein processing pathway and increased Aβ degrading enzymes in the hippocampus of SAMP8 mice. These results collectively demonstrate the neuroprotective role of these new I2-IR ligands in a mouse model of brain aging through specific pathways and suggest their potential as therapeutic agents in brain disorders and age-related neurodegenerative diseases.
Response to Reviewers:	As required by editorial manager before to resubmit our manuscript it was revised by Edanz professional editing service (https://www.edanzediting.com/). Moreover we avoid depression, anxiety etc mention in the final version as suggested by Dr Mouradian.

Behavioral and cognitive improvement induced by novel imidazoline I_2 receptor ligands in female SAMP8 mice

Christian Griñán-Ferré,[†,○] Foteini Vasilopoulou,[†,○] Sònia Abás,[‡] Sergio Rodríguez-Arévalo,[‡] Andrea Bagán,[‡] Francesc X. Sureda,[§] Belén Pérez,[ǀ] Luis F. Callado,[¶] Jesús A. García-Sevilla,[#] M. Julia García-Fuster,[#] Carmen Escolano,[‡] and Mercè Pallàs[†,*]

[†]Pharmacology Section. Department of Pharmacology, Toxicology and Medicinal Chemistry, Faculty of Pharmacy and Food Sciences, and Institut de Neurociències, University of Barcelona, Av. Joan XXIII, 27-31, E-08028 Barcelona, Spain.

[‡]Laboratory of Medicinal Chemistry (Associated Unit to CSIC), Department of Pharmacology, Toxicology and Medicinal Chemistry, Faculty of Pharmacy and Food Sciences, and Institute of Biomedicine (IBUB), University of Barcelona, Av. Joan XXIII, 27-31, E-08028 Barcelona, Spain.

[§]Pharmacology Unit, Faculty of Medicine and Health Sciences, University of Rovira and Virgili, C./St. Llorenç 21, E-43201 Reus, Tarragona, Spain.

[ǀ]Departament of Pharmacology, Therapeutic and Toxicology, Autonomous University of Barcelona E-08193, Spain.

[¶]Department of Pharmacology, University of the Basque Country, UPV/EHU, E-48940 Leioa, Bizkaia, and Centro de Investigación Biomédica en Red de Salud Mental, CIBERSAM, Spain.

[#]Laboratory of Neuropharmacology, IUNICS and IdISBa, University of the Balearic Islands (UIB), Cra. Valldemossa km 7.5, E-07122 Palma de Mallorca, Spain.

*Corresponding author:

Mercè Pallàs, PhD

pallas@ub.edu

Pharmacology Section. Department of Pharmacology, Toxicology and Medicinal Chemistry, Faculty of Pharmacy and Food Sciences, and Institut de Neurociències, University of Barcelona, Av. Joan XXIII, 27-31, E-08028 Barcelona, Spain.

Keywords: Imidazoline I_2 receptors, (2-imidazolin-4-yl)phosphonates, behavior, cognition, neurodegeneration, neuroprotection, aging.

ABSTRACT

As populations increase their life expectancy, age-related neurodegenerative disorders such as Alzheimer's disease have become more common. I_2-Imidazoline receptors (I_2-IR) are widely distributed in the central nervous system, and dysregulation of I_2-IR in patients with neurodegenerative diseases has been reported, suggesting their implication in cognitive impairment. This evidence indicates that high-affinity selective I_2-IR ligands potentially contribute to the delay of neurodegeneration. *In vivo* studies in the female senescence accelerated mouse-prone 8 mice have shown that treatment with I_2-IR ligands, **MCR5** and **MCR9**, produce beneficial effects in behavior and cognition. Changes in molecular pathways implicated in oxidative stress, inflammation, synaptic plasticity, and apoptotic cell death were also studied. Furthermore, treatments with these I_2-IR ligands diminished the amyloid precursor protein processing pathway and increased Aβ degrading enzymes in the hippocampus of SAMP8 mice. These results collectively demonstrate the neuroprotective role of these new I_2-IR ligands in a mouse model of brain aging through specific pathways and suggest their potential as therapeutic agents in brain disorders and age-related neurodegenerative diseases.

INTRODUCTION

Imidazoline receptors (non-adrenergic receptors for imidazolines) [1] have been identified as a promising biological target that deserves further investigation using multidisciplinary approaches to build a comprehensive understanding of their pharmacological possibilities. To date, three main imidazoline receptors, I_1-, I_2- and I_3-IR, have been identified as binding sites that recognize different radiolabeled ligands involving different locations and physiological functions [2-4]. The pharmacological characterization of I_1-IR is understood the best, and they are used in the antihypertensive drugs moxonidine [5] or rilmenidine [6]. To date, I_2-IR have not been structurally described, although García-Sevilla's group has defined distinct binding proteins corresponding to subgroups of I_2-IR sites [7]. I_2-IR are involved in analgesia [8] glial tumors [9], inflammation [10] and a plethora of brain disorders, such as AD [11,12], Parkinson's disease (PD) [13], and different psychiatric disorders [14-16]. The efficacy of the analgesic CR4056 in osteoarthritis has advanced this compound in the first-in-class I_2-IR ligand to achieve phase II clinical trials [17]. I_2-IR are widely distributed in the CNS, binds imidazoline-based compounds [18, 19], such as idazoxan or valldemossine [20], and have been associated with the catalytic site of monoamine oxidase enzyme (MAO) [21]. A neuroprotective role for I_2-IR was described through the pharmacological activities observed for their ligands [22]. Idazoxan reduced neuron damage in the hippocampus after global ischemia in the rat brain [23] and agmatine, identified as the endogenous I_2-IR ligand [24], has demonstrated modulatory actions in several neurotransmitters that produce neuroprotection both *in vitro* and in rodent models [25]. The compelling evidence has demonstrated that other selective I_2-IR ligands (Figure 1) provide benefits such as being neuroprotective against cerebral ischemia *in vivo* [26, 27], inducing beneficial effects in several models of chronic opioid therapy, leading to neuroprotection by direct blocking of *N*-methyl-D-aspartate receptor (NMDA) mediated intracellular [Ca^{2+}] influx [28], or provoking morphological/biochemical changes in astroglia that are neuroprotective after neonatal axotomy [22].

At a cellular level, I_2-IR are situated in the outer membrane of the mitochondria in astrocytes [29], and a direct physiological function of glial I_2-imidazoline preferring sites that regulate the level of the astrocyte marker glial fibrillary acidic protein (*Gfap*) has been proposed [30]. In addition, astrogliosis is a pathophysiological trend in brain neurodegeneration as in AD [31]. The density of I_2-IR is markedly increased in the brains of patients with AD [13], and in gliosis associated wiht brain injury [32].

The pharmacological characterization of these receptors relies on the discovery of selective I_2-IR ligands devoid of a high affinity for I_1-IR and α_2-adrenoceptors. The reported I_2-IR ligands are structurally restricted, featuring rigid substituted pattern imidazolines, and most of which are not entirely selective and thus interact with α-adrenoceptors [19], which causes side effects [33]. Our chemistry program aimed to find new selective I_2-IR ligands to increase the arsenal of pharmacological tools to exploit the therapeutic potential of I_2-IR in neuroprotection.

We have recently synthesized a series of new chemical scaffolds, 2-imidazolin-4-yl)phosphonates [34], by an isocyanide-based multicomponent reaction under microwave irradiation to avoid using solvents. The experimental synthetic conditions fulfill the principles of green chemistry, giving access to novel compounds with high selectivity and affinity for I_2-IR. Among them, we tested **MCR5** [diethyl (1-(3-chloro-4-fluorobenzyl)-5,5-dimethyl-4-phenyl-4,5-dihydro-1*H*-imidazol-4-yl)phosphonate] in previous work to demonstrate its neuroprotective and analgesic effects, and it showed promising results in models of brain damage [35]. In particular, mechanisms of neuroprotection related to regulating apoptotic pathways or inhibiting p35 cleavage mediated by this new active compound have been found. In the present work, we explored the behavioral and cognitive status, including molecular changes associated with age and neurodegenerative processes, presented by SAMP8 mice when treated with the new highly selective I_2-IR ligands **MCR5** and **MCR9** [methyl 1-(3-chloro-4-fluorobenzyl)-5,5-dimethyl-4-phenyl-4,5-dihydro-1*H*-imidazole-4-carboxylate] (Figure 2). SAMP8 is a naturally occurring mouse strain that displays a phenotype of accelerated aging with cognitive decline, as observed in AD, and is widely used as a feasible rodent model of cognitive dysfunction [36]. To the best of our knowledge, this manuscript reports the first study that includes cognitive and behavioral parameters of novel I_2-IR ligands in a well-characterized animal model for studying brain aging and neurodegeneration.

Material and methods

*Synthesis of I_2-IR ligands **MCR5** and **MCR9***

The compounds were prepared using our previously optimized conditions [34]. I_2-IR p*K*i for **MCR5** and **MCR9** were determined as 9.42±0.16 nM and 8.85±0.21 nM, respectively, showing that both compounds also had high selectivity against α_2 adrenergic receptors (457 and 1862, respectively) [35].

The blood-brain barrier (BBB) determination method

The *in vitro* permeability (Pe) of the novel compounds through a lipid extract of the porcine brain was determined using a mixture of PBS/EtOH 70:30. The concentration of drugs was determined using a UV/VIS (250-500 nm) plate reader. Assay validation was carried out by comparing the experimental and reported permeability values of 14 commercial drugs (see supporting information), which provided a good linear correlation: Pe (exp) = 1.003 Pe (lit) – 0.783 (R^2 = 0.93). Using this equation and the limits established by Di et al. [37] for BBB permeation, the following ranges of permeability were established: Pe (10^{-6} cm·s^{-1}) > 5.18 for compounds with high BBB permeation (CNS+); Pe (10^{-6} cm·s^{-1}) < 2.06 for compounds with low BBB permeation (CNS–); and 5.18 > Pe (10^{-6} cm·s^{-1}) > 2.06 for compounds with uncertain BBB permeation (CNS±).

Measurements of hypothermic effects

For this study, 25 adult male CD-1 mice (30-40 g) bred in the animal facility at the University of the Balearic Islands were used. Mice were housed in standard cages under defined environmental conditions (22°C, 70% humidity, and a 12-h light/dark cycle, lights on at 8:00 AM) and with free access to a standard diet and tap water. Experimental procedures followed the ARRIVE [38] and standard ethical guidelines (European Communities Council Directive 86/609/EEC and Guidelines for the Care and Use of Mammals in Neuroscience and Behavioral Research, National Research Council 2003) and were approved by the Local Bioethics Committee (UIB-CAIB). All efforts were made to minimize the number of mice used and their suffering.

Mice were handled and weighed by the same person for 2 days so they could habituate to the experimenter before any experimental procedures were initiated. For the acute treatment, mice received a single dose of **MCR9** (20 mg/kg, i.p., n=6) or vehicle (a mixture of equal parts of DMSO and saline, i.p., n=7). For the repeated treatment, mice were daily treated with **MCR9** (20 mg/kg, i.p., n=6) or vehicle (a mixture of equal parts of DMSO and saline, i.p., n=6) for 5 consecutive days. The hypothermic effect of compound **MCR9** was evaluated by measuring rectal temperature before any drug treatment (basal value) and 1 h after drug injection by a rectal probe connected to a digital thermometer (compact LCD thermometer, SA880-1M, RS, Corby, UK). Mice were sacrificed immediately after the last measurement of rectal temperature.

SAMP8 mouse in vivo experiments

SAMP8 female mice (n=26) (12 months old) were used to carry out cognitive and molecular analyses. We divided these animals randomly into three groups: SAMP8 Control (SP8-Ct, n=10) and SAMP8 treated with I_2-IR ligands (**MCR5**, n=8 and **MCR9**, n=8). Animals had free access to food and water and were kept under standard temperature conditions (22±2°C) and a 12-h light/dark cycle (300 lux/0 lux). **MCR5** and **MCR9** (5 mg/Kg/day) were dissolved in 1,8% 2-hydroxypropyl-β-cyclodextrin and administered through drinking water for 4 weeks. Water consumption was controlled each week, and I_2-IR ligand concentrations were adjusted accordingly to reach the optimal dose.

Studies and procedures involving mice brain dissection and subcellular fractionation were performed by the ARRIVE [38] and international guidelines for the care and use of laboratory animals (see above) and approved by the Ethics Committee for Animal Experimentation at the University of Barcelona.

Open field (OFT), elevated plus maze (EPM), and novel object recognition test (NORT)

The OFT apparatus was a white polywood box (50x50x25 cm). The floor was divided into two areas defined as center zone and peripheral zone (15 cm between the center zone and the wall). Behavior was scored with SMART® ver.3.0 software, and each trial was recorded for later analysis using a camera situated above the apparatus. Twenty-six mice (n=8-10 per group) were placed at the center and allowed to explore the box for 5 min. Afterward, the mice were returned to their home cages and the OFT apparatus was cleaned with 70% EtOH. The parameters scored included center staying duration, rears, defecations, and the distance traveled, calculated as the sum of total distance traveled in 5 min.

The EMP apparatus consists of opened arms and closed arms, crossed in the middle perpendicularly to each other, and a central platform (5×5cm) constructed of dark and white plywood (30×5×15 cm). To initiate the test session, 26 mice (n=8-10 per group) were placed on the central platform, facing an open arm, and allowed to explore the apparatus for 5 min. After the 5-min test, mice were returned to their home cages, and the

EPM apparatus was cleaned with 70% EtOH and allowed to dry between tests. Behavior was scored with SMART® ver.3.0 software, and each trial was recorded for later analysis using a camera fixed to the ceiling at a height of 2.1 m and situated above the apparatus. The parameters recorded included time spent on opened arms, time spent on closed arms, time spent in the center zone, rears, defecation and urination.

The NORT protocol employed was a modification of that of Ennaceur and Delacour [39]. In brief, 26 mice (n=8-10 per group) were placed in a 90°, two-arm, 25-cm-long, 20-cm-high, 5-cm-wide black maze. The walls could be removed for easy cleaning. Light intensity in mid-field was 30 lux. Before performing the test, the mice were individually habituated to the apparatus for 10 min for 3 days. On day 4, the animals were submitted to a 10-min acquisition trial (first trial), during which they were placed in the maze in the presence of two identical, novel objects (A+A or B+B) at the end of each arm. A 10-min retention trial (second trial) was carried out 2 h and 24 h later, with one of the two objects changed. During these second trials, mice behavior was recorded with a camera. The time with the new object (TN) and the time with the old object (TO) were measured. A discrimination index (DI) was defined as (TN−TO)/(TN+TO). The maze and the objects were cleaned with 96% EtOH after each test to eliminate olfactory cues.

Brain processing

Mice were euthanized by cervical dislocation 1 day after the behavioral and cognitive tests finished. Brains were immediately removed from the skull. The hippocampus of each mouse was then isolated and frozen in powdered dry ice. Each hippocampus was maintained at -80°C for further use. Tissue samples were homogenized in lysis buffer containing phosphatase and protease inhibitors (Cocktail II, Sigma-Aldrich). Total protein levels were obtained and the Bradford method was used to determine protein concentration.

Protein levels determination by western blot (WB)

For WB, aliquots of 15 µg of hippocampal protein were used. Protein samples from 15 mice (n=5 per group) were separated by SDS-PAGE (8%-12%) and transferred onto PVDF membranes (Millipore). Afterward, membranes were blocked in 5% non-fat milk in 0,1% Tween20 TBS (TBS-T) for 1 h at room temperature, followed by overnight incubation at 4°C with the primary antibodies listed in Table 1 (Supporting Information).

Membranes were washed and incubated with secondary antibodies for 1 h at room temperature. Immunoreactive proteins were viewed with a chemiluminescence-based detection kit, following the manufacturer's protocol (ECL Kit; Millipore) and digital images were acquired using a ChemiDoc XRS+ System (BioRad). Semi-quantitative analyses were carried out using ImageLab software (BioRad), and results were expressed in arbitrary units, considering control protein levels as 100%. Protein loading was routinely monitored by immunodetection of glyceraldehyde-3-phosphate dehydrogenase (GAPDH).

Determination of OS in the hippocampus

Hydrogen peroxide (H_2O_2) from 12 mice (n=4 per group) was measured in hippocampal tissue protein extracts obtained as described above. It was used as an indicator of OS and was quantified using a hydrogen peroxide assay kit (Sigma-Aldrich, St. Louis, MI) according to the manufacturer's instructions.

RNA extraction and gene expression determination

Total RNA isolation was carried out using the TRIzol® reagent according to manufacturer's instructions. The yield, purity, and quality of RNA were determined spectrophotometrically with a NanoDrop™ ND-1000 (Thermo Scientific) apparatus and an Agilent 2100B Bioanalyzer (Agilent Technologies). RNAs with 260/280 ratios and RIN higher than 1.9 and 7.5, respectively, were selected. Reverse Transcription-Polymerase Chain Reaction (RT-PCR) was performed as follows: 2 µg of mRNA was reverse-transcribed using the high capacity cDNA reverse transcription kit (Applied Biosystems). Real-time quantitative PCR (qPCR) was employed to quantify the mRNA expression of OS genes heme oxygenase (decycling) 1 (*Hmox1*), aldehyde oxidase 1 (*Aox1*), cyclooxygenase 2 (*Cox2*), inflammatory genes interleukin 6 (*Il-6*), interleukin 1 beta (*Il-1β*), tumor necrosis factor alpha (*Tnf-α*), amyloid processing gene disintegrin, and metalloproteinase domain-containing protein 10 (*Adam10*) and amyloid degradation gene neprilysin (*NEP*). The primers are listed in Table 2 (Supporting Information).

SYBR® Green real-time PCR was performed in a Step One Plus Detection System (Applied-Biosystems) employing SYBR® Green PCR Master Mix (Applied-Biosystems). Each reaction mixture contained 7.5 µL of cDNA (a 2-µg concentration), 0.75 µL of each primer (a 100-nM concentration, each), and 7.5 µL of SYBR® Green PCR Master Mix (2X).

TaqMan-based real-time PCR (Applied Biosystems) was also performed in a Step One Plus Detection System (Applied-Biosystems). Each 20 µL of TaqMan reaction contained 9 µL of cDNA (25 ng), 1 µL 20X probe of TaqMan Gene Expression Assays and 10 µL of 2X TaqMan Universal PCR Master Mix.

Data were analyzed using the comparative cycle threshold (Ct) method (ΔΔCt), where the housekeeping gene level was used to normalize differences in sample loading and preparation. Normalization of expression levels was performed with *actin* for SYBR® green-based real-time PCR results and *Tbp* for TaqMan-based real-time PCR. Each sample (n=4-5 per group) was analyzed in duplicate, and the results represent the n-fold difference of the transcript levels among different groups.

Statistical analysis

The statistical analyses were conducted using GraphPad Prism ver. 6 statistical software. Data were expressed as the mean ± standard error of the mean (SEM). Means were compared with one-way analysis of variance (ANOVA) and Tukey's post hoc test or two-tailed Student's *t*-test when necessary. Statistical significance was considered when *p* values were <0.05. Statistical outliers were performed out with Grubbs' test and were removed from the analysis.

RESULTS

BBB permeation assay for I_2-IR ligands MCR5 and MCR9

The tested compounds **MCR5** and **MCR9** had Pe values of 13.5±0.9 and 26.9±1.7, respectively, well above the threshold for high BBB permeation, so they were predicted to be able to cross the BBB and reach their biological target in the CNS. Supplementary information on results analysis can be found in the supporting material (Table 3).

Hypothermic effects of MCR9 in mice

Selective I_2-IR ligands induce hypothermia in rodents [4]. In particular, the hypothermic effect of compound **MCR5** in mice was evaluated in a recent study from our research group (results for compound **2c** in ref 35) [35]. Similar to **MCR5**, **MCR9** induced mild hypothermia as assessed by a moderate reduction (-2.3°C) in rectal temperature 1 h after injection at the tested dose of 20 mg/kg in adult CD-1 mice and as compared with vehicle-treated controls (Figure 3A, day 1). While repeated (5 days) administration (20 mg/kg) revealed persistent the hypothermic effects of **MCR9** from days 1 to 4 (range from -2.3 to -3.2°C), on day 5 no significant change was observed in body temperature (-1.8°C change) as compared with vehicle-treated controls (Figure 3B).

Beneficial effects on behavior and cognition induced by MCR5 and MCR9 in SAMP8 mice

Results obtained in OFT demonstrated that both compounds increased locomotor activity and time spent in the center zone (Figure 4A and B). Furthermore, a significant increment in the vertical activity, quantified by the number of total rears, was observed in mice treated with **MCR5** or **MCR9** in OFT and the EPM (Figure 4C and F). EPM data indicated a reduction in anxiety-like behavior by a significant decrease in time spent in closed arms for treated animals compared with controls (Figure 4E). These results are supported by a preference for opened arms, although not significant, for **MCR5** (Figure 4D). Moreover, a significant increase in the DI indicates an improved performance in recognition of the new object in the NORT between **MCR5**- and **MCR9**-treated SAMP8 mice compared with the control group. A robust effect in short (2 h) and long-term (24 h) memory was found for the two tested compounds (Figure 4G and H).

OS and inflammatory markers reduced by MCR5 and MCR9 in SAMP8 mice

OS and neuroinflammation are thought to be key risk factors in the development of neurodegeneration. The hydrogen peroxide levels in the hippocampus were significantly reduced in brains of mice treated with either **MCR5** or **MCR9** compared with the control group (Figure 5A). Of note, superoxide dismutase 1 (SOD1) protein levels in treated mice were reduced by **MCR5** but not by **MCR9** (Figure 5B). Moreover, *Hmox1* gene expression, an important key enzyme in cellular antioxidant-defense, was also significantly increased with both **MCR5** and **MCR9** (Figure 5D). Other OS markers, such as *Aox1* or *Cox2*, were not significantly altered (Figure 5D). Regarding the inflammation markers, no changes were observed in *Il-6* gene expression for tested compounds, but a significant decrease in *Il-1β* and *Tnf-α* for **MCR5** treated SAMP8 mice was found (Figure 5E). Moreover, a significant diminution in *Gfap* gene expression was determined, reinforcing the prevention of inflammatory processes by **MCR5** and **MCR9** (Figure 5C).

Changes in synaptic markers and apoptotic factors induced by MCR5 and MCR9 in SAMP8 mice

MCR5, but not **MCR9**, induced an increase in postsynaptic density protein 95 (PSD95) protein levels (Figure 6A). Protein levels for synaptophysin (SYN), a presynaptic protein, showed a slight increase for both compounds, although it did not reach significance (Figure 6B). To determine the implication of proteolytic processes in the **MCR5** and **MCR9** compounds, we found reduced levels of calpain (data not shown) with a significant diminution in 150 α-spectrin breakdown fragment (SPBD) (Figure 6C). Furthermore, **MCR9** and **MCR5** reduced caspase-3 activity in SAMP8 mouse hippocampi, because of the diminution of caspase-3 protein levels and 120 SPBD fragments, which reached significance for **MCR9** (Figure 6C and D). Moreover, B-cell lymphoma 2 (Bcl-2) levels were diminished, and Bcl-2-associated X (Bax), a key protein in the apoptotic cascade, was reduced by **MCR5** (Figure 6E and F), supporting a possible implication of I_2-IR in apoptosis processes.

Changes in mitogen-activated protein kinase (MAPK) signaling pathways reduced hyperphosphorylation of Tau induced by MCR5 and MCR9 in SAMP8 mice

Key proteins associated with molecular pathways disturbed in brain disorders and neurodegeneration were evaluated by WB. Interestingly, **MCR5**, but not **MCR9**, increased the p-AKT/AKT ratio (protein kinase B) (Figure 7A). Accordingly, higher levels of inactivated glycogen synthase kinase 3 beta (GSK3β), phosphorylated in Ser9, were determined (Figure 7B). Extracellular signal-regulated kinase (ERK½) inhibition by **MCR5** and **MCR9** was demonstrated by a reduction of the p-ERK½ ratio (Figure 7C). Furthermore, cyclin-dependent kinases 5 (CDK5) measured by the p-CDK5/CDK5 and p25/p35 ratios were also reduced (Figure 7D and E). Taking into account the results obtained on kinases CDK5, GSK3β, AKT, and ERK½, we studied Tau hyperphosphorylation levels in the hippocampi of SAMP8 mice. A significant reduction in Tau phosphorylation in treated SAMP8 mice was found, specifically for the Ser404 phosphorylation site, whereas the Ser396 phosphorylation site was reduced without reaching significance (Figure 7F).

Changes in APP processing and Aβ degradation induced by MCR5 and MCR9 in SAMP8 mice

We found a significant increase in sAPPα protein levels in **MCR9** treated SAMP8 mice (Figure 8A) and a significant reduction in sAPPβ protein levels in **MCR5** treated SAMP8 mice (Figure 8B). Furthermore, a significant increase in gene expression for *Adam10*, an α-secretase that cleaves APP and *NEP*, an Aβ degrading enzyme (Figure 8C and D) was observed in both treated mice groups compared with that in non-treated animals.

DISCUSSION

I_2-IR are related to several physiological and pathological processes, including those of the CNS, such as pain [8], neuropathic pain [40], seizures [41, 42], and neurodegenerative diseases such as AD [14, 43]. Our lab has a research line on developing new high affinity and selectivity I_2-IR ligands, maintaining the imidazoline scaffold and incorporating several substituents in the imidazoline ring. Some of these were previously tested for their neuroprotective role [35].

Given the enormous potential of I_2-IR and their implications in brain disorders and neurodegenerative diseases such as AD, we set out to explore whether **MCR5** and **MCR9**, two members of a structurally new family of I_2-IR ligands, might improve the behavioral and cognitive status in SAMP8 model mice. The main chemical structural differences were a phosphonate substituent on the imidazoline ring for **MCR5** in contrast with an ester group for **MCR9** (Figure 2).

Published results from our lab demonstrated that **MCR5** presented a p*K*i for the I_2-IR of 9.42±0.16 and high selectivity when compared with the α_2 receptor affinity [35]. Likewise, **MCR9** is a high-affinity I_2-IR ligand (p*K*i 8.85±0.21) but with a higher selectivity against α_2 receptors. Both **MCR5** and **MCR9** were predicted to be able to cross the BBB, an important drug characteristic when action is expected in the CNS.

Previous studies have evaluated the effects of selective I_2-IR ligands on inducing hypothermia in rodents [e.g., idazoxan or BU224] [44]. Accordingly, **MCR5** can induce hypothermia in mice, and showed a neuroprotective role in kainate-induced seizures, modifying levels of a Fas-associated protein with death domain (FADD) receptor [35]. While acute **MCR5** (5 and 20 mg/kg) induced mild hypothermia, repeated (20 mg/kg, 5 days) administration of **MCR5** revealed significantly attenuated hypothermic effects from day 2, which indicated the induction of tolerance to the hypothermic effects of the drug [35]. For **MCR9**, repeated (20 mg/kg, 5 days) administration revealed persistent hypothermic effects up to day 4. These results suggest that the slow induction of tolerance to the hypothermic effects caused by **MCR9** might be started following 5 days of drug administration, although a more extended treatment paradigm might be needed for confirmation.

The hypothermic effects exerted by **MCR5** and **MCR9** might be relevant to induce neuroprotection because it was previously proposed for some of the neuroprotective effects induced by the I_2-IR selective ligand idazoxan. Several experiments have ascertained a possible role for hypothermia in mediating neuroprotection. For example, small drops in temperature exerted neuroprotection in cerebral ischemia [45] and are typically used in the clinic to improve the neurological outcome under various pathological conditions (e.g., stroke, brain injury). Although the mechanisms explaining the neuroprotective effects mediated by hypothermia are not well understood, some researchers have suggested that they might be related to the inhibition of glutamate release [46].

SAMP8 mice have been studied as a non-transgenic murine mouse model of accelerated senescence and late-onset AD. These mice exhibit cognitive and emotional disturbances, probably due to the early development of pathological brain hallmarks, such as OS, inflammation, and activation of neuronal death pathways, which mainly affect the cerebral cortex and hippocampus [47, 48]. To date, this rodent model has not been used to test I_2-IR ligands. Thus, this work is the first investigation of the effects of the improvement of cognitive impairment and behavior in this mouse model after treatment with I_2-IR ligands.

Behavioral and cognitive effects were investigated through three well-established tests in SAMP8 mice: the OFT, which is an experiment used to assay general locomotor activity and anxiety in rodents [49]; the EPM, one of the most widely used tests for measuring anxiety-like behavior [50]; and the NORT, as a standard measure of cognition (for short- and long-term memory) [51].

The OFT and EPM parameters indicated a reduction in cognitive impairment through showing improved locomotor activity jointly with an anti-anxiousness effect. Likewise, the NORT results demonstrated an improvement in cognitive and short- and long-term learning capabilities in hippocampal memory processes. Therefore, all the assessed parameters showed robust beneficial effects on cognition and behavior after **MCR5** and **MCR9** treatment in SAMP8 mice.

The results in cognitive and behavioral effects were supported by a cellular and biochemical assessment of characteristic parameters related to cognitive decline and AD. The compelling evidence demonstrated a neuroprotective role for I_2-IR. The neuroprotective role can be related to OS and inflammation [52] by measuring OS indicators and inflammation markers in SAMP8 mouse brain tissue treated with the I_2-IR ligands, **MCR5** and **MCR9**. Results showed significant reduced hydrogen peroxide levels in hippocampal tissue and increased *Hmox1* gene expression in treated **MCR5** and **MCR9** SAMP8 mice, but not in other sensors for OS, such as *Aox1* or *Cox2*. SOD1 protein levels were reduced by **MCR5** but not by **MCR9**. Regarding inflammation markers, no changes were observed in *Il-6* gene expression for tested compounds, but a significant decrease in *Il-1β* and *Tnf-α* for **MCR5** treated SAMP8 mice was found. In addition, reduced astrogliosis was found in treated animals, corroborating a reduced inflammatory environment in hippocampi of **MCR5** and **MCR9** treated SAMP8 mice. Altogether these results showed a relatively weak influence in OS and inflammation mechanisms by I_2-IR ligands in SAMP8 mice [53-57]. However, a role for those two pathological conditions related to I_2-IR ligand interaction cannot be discarded because **MCR5** elicited beneficial effects despite the old age of the SAMP8 mice. Aged SAMP8 mice present lower inflammation and OS due to being at the endpoint of the senescence process [56, 57]. Therefore, it can be challenging to determine drug effects on these processes in aged SAMP8 mice.

MCR5 and **MCR9** effects on key molecular markers for synapsis and apoptosis were studied to unravel the prevention of cognitive decline by I_2-IR ligands in SAMP8 mice, which is characterized by alterations in those processes. In consonance with better cognitive performance, the compounds tested increased synaptic markers such as SYN and PSD95, indicating a neuroprotective role for **MCR5** and **MCR9**.

There are several cellular and molecular pathways related to better synaptic performance, including proteolytic and phosphorylation activities or apoptotic processes. Regarding proteolytic processes, calpain is an intracellular protease that cleaves the CDK5 activator p35 to a p25 fragment**. MCR5** and **MCR9** diminished calpain levels and its activity with a reduced 150 SPBD fragment. Moreover, a significant reduction in p25 protein levels was found in treated SAMP8 mice. A decrease in p25 can also influence CDK5 activity, as implicated in Tau phosphorylation [58, 59]. These results indicate that CDK5 phosphorylation activity should be diminished after I_2-IR ligand treatment, corroborating results obtained previously for **MCR5** in a kainate model of neuronal damage [60].

Caspase 3 mediated apoptosis was also addressed. A significant reduction of caspase 3 activity and diminution of Bax protein were found in **MCR9** treated SAMP8 mice. Because Bax is described as a pro-apoptotic protein, its diminution indicates a possible protective role for I_2-IR ligands in neurons [61]. By contrast, reduced levels of Bcl-2, considered an anti-apoptotic protein, deserve further studies. Several authors have indicated that when Bax is reduced, Bcl-2 is less necessary for blocking Bax dimer to form the mitochondrial pore; in this situation cells reduce the Bcl-2 levels as a control mechanism [62].

An increase in p-AKT was induced by the I_2-IR ligands, whereas a decrease in ERK½ activation was observed. p-AKT inactivated GSK3β, a key kinase involved in the process of Tau hiperphosphorylation, by phosphorylation in Ser9. To this point, **MCR5** and **MCR9** treated SAMP8 mice showed an increase of Ser9 phosphorylated GSK3β and reduced Tau hyperphosphorylation.

ERK½ inhibition (that reduction of p42/p44) by **MCR5** and **MCR9** can contribute to the beneficial effect elicited by I_2-IR on synaptic markers and Tau phosphorylation processes. ERK½ belongs to a subfamily of MAPKs and plays diverse roles in the CNS, such as neuronal survival or death, synaptic plasticity, and learning and memory through phosphorylation of regulatory enzymes and kinases [63, 64]. Although crucial for neuronal survival, there is some evidence that prolonged activation of the ERK pathway can induce a deleterious effect to the cell [65, 66]. Interestingly, long-lasting ERK activation in neurons has been demonstrated in neurodegenerative diseases such as AD [67, 68] and PD [69]. Here, the inhibition of this kinase participates in post-translational modifications in cytoskeletal proteins such as Tau, ameliorating the neuronal network functioning, as demonstrated with an increase in synaptic markers.

The relationship among MAPKs, such as ERK½, [70] and PI3K, such as AKT, and imidazoline receptors is well defined [71, 72]. In this respect, it has been described that either ERK or AKT can be associated with the multifunctional *Fas*/*FADD* complex [73, 74]. Apoptosis is an important contributor to neurodegeneration [75], and in this regard, the FADD protein has been suggested as a putative biomarker for pathological processes associated with the course of clinical dementia [76]. It has been reported that total FADD has a central role in promoting apoptosis [77, 78] and its phosphorylation at Ser191/194 mediates non-apoptotic actions such as cell growth and differentiation [79]. In our previous work, we demonstrated that **MCR5** modified FADD phosphorylation (i.e., it increased the p-FADD/FADD ratio) in a kainate-treated rat model [35]. These results could explain the modulation of proteins from the apoptotic pathway mentioned before (e.g., a diminution in caspase 3 activation and significant changes in Bcl-2 and Bax), which seems to favor anti-apoptotic actions mediated through I_2-receptors, and especially by **MCR5**.

Tau hyperphosphorylation is a histological trend in many neurodegenerative diseases characterized by cognitive decline, including AD. Therefore we studied APP processing pathways. Aberrant APP processing is a hallmark of cognitive decline diseases [80]. To assess the capacity of the tested compounds to modify this pathological hallmark, we evaluated APP fragments, specifically, sAPPα and sAPPβ. Despite neither APP fragment reaching significance in either I_2-IR ligand treated SAMP8 mice group, we found a clear tendency, which indicates the non-amyloidogenic pathway preference. Moreover, sAPPα is described as a neuroprotective, neurotrophic and cell excitable regulator with synaptic plasticity [81]. *Adam10* [82] and *NEP* [83] gene expression were higher in **MCR5** and **MCR9** treated mice groups than in non-treated animals. In sum, I_2-IR ligands foster a diminution in the amyloidogenic pathway and higher degradation of β-amyloid in the SAMP8 mice model.

In conclusion, the effectiveness of the two new I_2-IR ligands in an *in vivo* female model for cognitive decline was demonstrated in this study. SAMP8 model mice are gated to neurodegenerative processes, such as AD, and our research has shown that **MCR5** and **MCR9** can open new therapeutic avenues against these pathological conditions that currently have unmet medical needs. Although different authors have previously indicated the relationship between I_2-IR and cognitive decline, this study is the first experimental evidence that demonstrates the possibility of using this receptor as a target for cognitive impairment. Here, we demonstrate that this strategy could represent a future approach to treating devastating conditions such as AD.

Author Contributions

C. G.-F. and F. V. contributed equally. C. G.-F., C. E., L. F. C. and M. P. designed the study. B. P. performed the PAMPA-BBB permeation experiments. C. G.-F. and F. V. carried out the behavior and cognition studies and cellular parameters determination (OS and inflammation markers, synaptic markers and apoptotic factors, and hyperphosphorylation of Tau). J. A. G.-S. and M. J. G.-F. performed the hypothermic studies. S. A., S. R.-A. and A. B. synthesized and purified the l_2-IR ligands. C. G.-F., L.

F. C., F. X. S., J. A. G.-S., M. J. G.-F., C. E. and M. P. contributed to writing the manuscript. All authors have read and approved the final version of the manuscript.

Acknowledgments

This study was supported by Ministerio de Economía y Competitividad of Spain (SAF2016-33307 and SAF2014-55903-R) and the Basque Government (IT616/13). C. G.-F., F. V., F. X. S., C. E. and M. P. belong to 2017SGR106 (AGAUR, Catalonia). J. A. G.-S. is a member emeritus of the Institut d'Estudis Catalans (Barcelona, Catalonia). Financial support was provided for F. V. (University of Barcelona, APIF_2017), S. R.-A. (Generalitat de Catalunya, 2018FI_B_00227) and A. B. (Institute of Biomedicine UB_2018).

ABBREVIATIONS

AD, Alzheimer's disease; *Adam10*, A disintegrin and metalloproteinase domain-containing protein 10; ANOVA, one-way analysis of variance; APP, amyloid precursor protein; *Aox1*, aldehyde oxidase 1; AKT, protein kinase B; Bcl-2, B-cell lymphoma 2; Bax, Bcl-2-associated X; BBB, blood-brain barrier; CDK5, cyclin-dependent kinase 5; CNS, central nervous system; *Cox2*, cyclooxygenase 2; Ct, cycle threshold; DI, discrimination index; EPM, elevated plus maze; ERK, extracellular signal-regulated kinase; GAPDH, glyceraldehyde-3-phosphate dehydrogenase; FADD, Fas-associated protein with death domain; *Gfap*, glial fibrillary acidic protein; GSK3β, glycogen synthase kinase 3 beta; *Hmox1*, heme oxygenase (decycling) 1; I_2-IR, I_2-Imidazoline receptors; *Il-1β*, interleukin 1 beta; *Il-6*, interleukin 6; MAO, monoamine oxidases; MAPK, mitogen-activated protein kinase; *NEP*, neprilysin; NMDA, *N*-methyl-D-aspartate; NORT, novel object recognition test; OFT, open field test; OS, oxidative stress; PCR, polymerase chain reaction; PD, Parkinson's disease; Pe, permeability; PI3K, phosphatidylinositol-4,5-bisphosphate 3-kinase; PSD95, postsynaptic density protein 95; SAMP8, senescence accelerated mouse prone 8; SPBD, spectrin breakdown; SEM, standard error of the mean; SOD1, superoxide dismutase 1; SYN, synaptophysin; TBP, tata-binding protein; TN, time with new object; *Tnf-α*, tumor necrosis factor alpha; TO, time with old object; WB, western blot.

Figure 1. Representative I_2-IR ligands.

Figure 2. Structure of I_2-IR ligands **MCR5** and **MCR9**.

Figure 3. Acute and repeated measurement of the hypothermic effect of compound **MCR9** in mice. (A) Effect of acute treatment with **MCR9** (20 mg/kg, i.p.) on rectal body temperature in mice. Columns are means ± SEM of the difference (Δ, 1 h - basal value) in body temperature (°C) for **MCR9**-treated mice compared with vehicle-treated **Control** mice. Data were analyzed using Student's t-test. **p<0.01. (B) Effect of repeated (5 days) treatments with **MCR9** (20 mg/kg, i.p., closed circles) on rectal body temperature in mice. Circles are means ± SEM of the difference (Δ, 1 h - basal value) in body temperature (°C) for **MCR9**-treated mice compared with vehicle-treated **Controls**. Data were analyzed using repeated measures ANOVA followed by Sidak's multiple comparison test. **p<0.01, ***p<0.001; (n=6-7 animals per group).

Figure 4. Behavioral and cognitive improvement in 12-month-old treated SAMP8 mice with both I_2-IR ligands. (A) A significant increase in the distance traveled in the open field test in the I_2-IR ligand treated groups compared with the **Control** group. (B) A significant increase in the percentage of time in the center zone of the opened field test in the **MCR5** treated group compared with the **Control** group, and no significant difference between the **MCR9** and **Control** groups. (C) A significant increase in the number of total rears of the opened field test among groups. (D) The time spent in the opened arms of the EPM did not differ among groups. (E) A significant increase in the time spent in the closed arms among the **Control** group compared with the treated groups. (F) A significant increase in the number of total rears of the EPM in the **MCR5** group compared with the **Control** group. (G) The results of the NORT in the short-term memory (2 h) revealed a significant increase in both I_2-IR ligand treated groups compared with the **Control** group as well as a significant reduction in the DI of the **MCR9** group compared with **MCR5** group, and (H) a significant increase in the DI of the long-term memory (24 h) in both I_2-IR ligand treated groups compared with the **Control** group. Data expressed as means ± SEM (n=8-10 animals per group) and analyzed using one-way ANOVA followed by Tukey's post hoc test for multiple comparisons. *p<0.05, **p<0.01, ***p<0.001 and ****p<0.0001.

Figure 5. Reduced OS and inflammatory markers in 12-month-old treated SAMP8 mice with both I_2-IR ligands. (A) There was a significant reduction in the hydrogen peroxide concentration in both I_2-IR ligand treated groups compared with the **Control** group in homogenates of the hippocampus tissue**.** (B) A significant reduction in SOD1 protein levels in the **MCR5** group compared with the **Control** group and no difference between the **MCR9** and **Control** groups. (C) A significant reduction in *Gfap* protein levels in the **MCR5** and **MCR9** groups compared with the **Control** group. (D) Gene expression of antioxidant enzymes in the mouse hippocampus. A significant increase in *Hmox1* gene expression, but not for *Aox1* and *Cox2,* among both I_2-IR ligand treated groups and the **Control** group. (E) A significant reduction in gene expression of *Il-1β* and *Tnf-α* in the **MCR5** group compared with the **Control** group, and a tendency for the same genes to reduce in the **MCR9** group. However, *Il-6* gene expression did not differ among groups. Values in bar graphs are adjusted to 100% for protein level of the **Control** group. Gene expression levels were determined by real-time PCR. Data are expressed as means ± SEM (n=4-5 animals per group) and analyzed using one-way ANOVA followed by Tukey's post hoc test for multiple comparisons. *p<0.05.

Figure 6. Changes in synaptic markers and apoptotic factors in 12-month-old treated SAMP8 mice with both I_2-IR ligands. (A) A significant increase in PSD95 protein levels in the **MCR5** group compared with the other two groups. (B) A tendency for SYN protein levels to increase in both I_2-IR ligand treated groups compared with the **Control** group. (C) A tendency for a reduction in the spectrin fragment SPBD 150, and a significant reduction in the spectrin fragment SPBD 120 in the **MCR9** group compared with the **Control** group. (D) A significant reduction in Caspase-3 protein levels in both I_2-IR ligand groups compared with the **Control** group. (E) A significant reduction in Bcl-2 protein levels in both I_2-IR ligand groups compared with the **Control** group. (F) A significant reduction in Bax protein levels in the **MCR9** group compared with the other groups. Values in bar graphs are adjusted to 100% for protein level of the **Control** group. Representative WB for each protein in the mouse hippocampus is shown. Data are expressed as means ± SEM (n=5 animals per group) and analyzed using one-way ANOVA followed by Tukey's post hoc test for multiple comparisons. *p<0.05, **p<0.001.

Figure 7. Changes in kinase signaling pathways reduced hyperphosphorylation of Tau in 12-month-old SAMP8 mice treated with both I_2-IR ligands. (A) A significant increase in the p-AKT ratio in the **MCR5** group compared with the other two groups. (B) A significant increase in inactive p-GSK3β (Ser9) protein levels in both I_2-IR ligand treated groups compared with the **Control** group. (C) A significant reduction in p-ERK½ in both I_2-IR ligand treated groups compared with the **Control** group. (D) Changes in the p-CDK5/CDK5 ratio induced by **MCR5** and **MCR9** treatment. (E) Changes in the p25/p35 ratio in the **MCR5** and **MCR9** groups compared with the **Control** group. Representative WB are shown. (F) A reduction in p-Tau (Ser396), as well as a significant reduction in p-tau (Ser404) in both I_2-IR ligand treated groups compared with the **Control** group. Values in bar graphs are adjusted to 100% for protein level of the **Control** group. Data are expressed as means ± SEM (n=5 animals per group) and analyzed using one-way ANOVA followed by Tukey's post hoc test for multiple comparisons. *$p<0.05$, **$p<0.01$, ***$p<0.001$.

Figure 8. Changes in APP processing and Aβ degradation enzymes in 12-month-old SAMP8 mice treated with both I_2-IR ligands. Representative WB of the APP and its fragments. (A) A significant increase in sAPPα protein levels in the **MCR9** group compared with the **Control** group, and no significant difference between the **MCR5** and **Control** groups. (B) A significant reduction in sAPPβ protein levels in the **MCR5** group compared with the **Control** group, and no significant difference between the **MCR9** and **Control** groups. (C) A significant increase in *Adam10* gene expression in the **MCR5** group compared with the **Control** group, and no significant difference in the **MCR9** group. (D) A significant increase in *NEP* gene expression in the **MCR5** group compared with the **Control** group, and no significant difference in the **MCR9** group. Values in bar graphs were adjusted to 100% for protein level of the **Control** group. Gene expression levels were determined by real-time PCR. Data are expressed as means ± SEM (n=4-5 animals per group) and analyzed using one-way ANOVA followed by Tukey's post hoc test for multiple comparisons. *$p<0.05$.

Behavioral and cognitive improvement induced by novel imidazoline I_2 receptor ligands in female SAMP8 mice

Christian Griñán-Ferré,[†,○] Foteini Vasilopoulou,[†,○] Sònia Abás,[‡] Sergio Rodríguez-Arévalo,[‡] Andrea Bagán,[‡] Francesc X. Sureda,[§] Belén Pérez,[ǀ] Luis F. Callado,[¶] Jesús A. García-Sevilla,[#] M. Julia García-Fuster,[#] Carmen Escolano,[‡] and Mercè Pallàs[†,*]

[†]Pharmacology Section. Department of Pharmacology, Toxicology and Medicinal Chemistry, Faculty of Pharmacy and Food Sciences, and Institut de Neurociències, University of Barcelona, Av. Joan XXIII, 27-31, E-08028 Barcelona, Spain.

[‡]Laboratory of Medicinal Chemistry (Associated Unit to CSIC), Department of Pharmacology, Toxicology and Medicinal Chemistry, Faculty of Pharmacy and Food Sciences, and Institute of Biomedicine (IBUB), University of Barcelona, Av. Joan XXIII, 27-31, E-08028 Barcelona, Spain.

[§]Pharmacology Unit, Faculty of Medicine and Health Sciences, University of Rovira and Virgili, C./St. Llorenç 21, E-43201 Reus, Tarragona, Spain.

[ǀ]Departament of Pharmacology, Therapeutic and Toxicology, Autonomous University of Barcelona E-08193, Spain.

[¶]Department of Pharmacology, University of the Basque Country, UPV/EHU, E-48940 Leioa, Bizkaia, and Centro de Investigación Biomédica en Red de Salud Mental, CIBERSAM, Spain.

[#]Laboratory of Neuropharmacology, IUNICS and IdISBa, University of the Balearic Islands (UIB), Cra. Valldemossa km 7.5, E-07122 Palma de Mallorca, Spain.

*Corresponding author:

Mercè Pallàs, PhD

pallas@ub.edu

Pharmacology Section. Department of Pharmacology, Toxicology and Medicinal Chemistry, Faculty of Pharmacy and Food Sciences, and Institut de Neurociències, University of Barcelona, Av. Joan XXIII, 27-31, E-08028 Barcelona, Spain.

Keywords: Imidazoline I_2 receptors, (2-imidazolin-4-yl)phosphonates, behavior, cognition, neurodegeneration, neuroprotection, aging.

ABSTRACT

As populations increase their life expectancy, age-related neurodegenerative disorders such as Alzheimer's disease (AD) have become more common. I_2-Imidazoline receptors (I_2-IR) are widely distributed in the central nervous system (CNS), and dysregulation of I_2-IR in patients with neurodegenerative diseases have been reported, suggesting their implication in cognitive impairment. This evidence supports that potential high-affinity selective I_2-IR ligands could contribute to the delay of the neurodegeneration. *In vivo* studies in the female Senescence Accelerated Mouse-Prone 8 mice (SAMP8) showed that treatments with our previously reported I_2-IR ligands, **MCR5** and **MCR9**, produce beneficial effects in behavior and cognition. Besides, changes in molecular pathways implicated in oxidative stress (OS), inflammation, synaptic plasticity, and apoptotic cell death were studied. Additionally, treatments with these I_2-IR ligands diminished the amyloid precursor protein (APP) processing pathway and increased Aβ degrading enzymes in the hippocampus of SAMP8 mice. Thus, altogether these results demonstrate the neuroprotective role for these new I_2-IR ligands through specific pathways, being promising therapeutic agents in brain disorders and age-related neurodegenerative diseases.

INTRODUCTION

Imidazoline receptors (non-adrenergic receptors for imidazolines) [1] have been identified as one of the promising biological targets that deserve further investigation by using multidisciplinary build comprehensive understanding of their pharmacological possibilities. To date, three main imidazoline receptors have been identified, namely I_1, I_2 and I_3-IR, as binding sites that recognize different radiolabelled ligands involving different locations, and physiological functions [2-4]. The pharmacological characterization of I_1-IR is understood the best yielding antihypertensive drugs moxonidine [5] or rilmenidine [6]. To date, I_2-IR have not been structurally described although the group of García-Sevilla has defined distinct binding proteins corresponding to subgroups of I_2-IR sites [7]. I_2-IR are involved in analgesia [8] glial tumors [9], inflammation [10] and in a plethora of brain disorders [11, 12], including AD [13,14] and Parkinson's disease (PD) [15], and different psychiatric disorders [16]. The efficacy of the analgesic CR4056 in osteoarthritis has advanced this compound in the first-in-class I_2-IR ligand to achieve phase II clinical trials [17]. I_2-IR are widely distributed in the CNS, binds imidazoline-based compounds [18, 19] as idazoxan or valldemossine [20], and have been associated with the catalytic site of monoamine oxidase enzyme (MAO) [21]. A neuroprotective role for I_2-IR was described through the pharmacological activities observed for their ligands [22]. Idazoxan reduced neuron damage in the hippocampus after global ischemia in the rat brain [23] and agmatine, identified as the endogenous I_2-IR ligand [24], has demonstrated modulatory actions in several neurotransmitters that produce neuroprotection both *in vitro* and in rodent models [25]. The compelling evidence has demonstrated that other selective I_2-IR ligands (Figure 1) are neuroprotective against cerebral ischemia *in vivo* [26, 27], induce beneficial effects in several models of chronic opioid therapy, lead to neuroprotection by direct blocking of *N*-methyl-D-aspartate receptor (NMDA) mediated intracellular [Ca^{2+}] influx [28], or provoke morphological/biochemical changes in astroglia that are neuroprotective after neonatal axotomy [22], amongst others.

At a cellular level, I_2-IR are situated in the outer membrane of mitochondria in astrocytes [29], and a direct physiological function of glial I_2-imidazoline preferring sites in the regulation of the level of the astrocyte marker Glial fibrillary acidic protein (*Gfap*) has been proposed [30]. Besides, it is widely known that astrogliosis is a pathophysiological trend in brain neurodegeneration as in AD [31]. The density of I_2-IR is markedly increased in the brains of patients with AD [13], as increases in the brain after gliosis [32].

The pharmacological characterization of these receptors relies on the discovery of selective I_2-IR ligands devoid of high affinity for I_1-IR and α_2-adrenoceptors. The reported I_2-IR ligands are structurally restricted featuring rigid substituted pattern imidazolines, and most of them are not entirely selective and interact also with α-adrenoceptors [19] and causing side effects [33]. Our chemistry program aimed to find new selective I_2-IR ligands to increase the arsenal of pharmacological tools to exploit the therapeutic potential of I_2-IR in neuroprotection.

Thus**,** we have recently synthesized a series of new chemical scaffolds, 2-imidazolin-4-yl)phosphonates [34], by an isocyanide-based multicomponent reaction under microwave irradiation avoiding the use of solvents. The experimental synthetic conditions fulfill the principles of green chemistry giving access to novel compounds with high selectivity and affinity for I_2-IR. Among them, we tested **MCR5** [diethyl (1-(3-chloro-4-fluorobenzyl)-5,5-dimethyl-4-phenyl-4,5-dihydro-1*H*-imidazol-4-yl)phosphonate] in previous work to demonstrate neuroprotective and analgesic effects, showing promising results in models of brain damage [35]. In particular, mechanisms of neuroprotection related to regulation of apoptotic pathways or inhibition of p35 cleavage mediated by this new active compound have been found. In the present work, we explored the behavioral and cognitive status, including molecular changes associated with age and neurodegenerative processes presented by SAMP8 when treated with these new highly selective I_2-IR ligands **MCR5** and **MCR9** [methyl 1-(3-chloro-4-fluorobenzyl)-5,5-dimethyl-4-phenyl-4,5-dihydro-1*H*-imidazole-4-carboxylate] (Figure 2). SAMP8 is a naturally occurring mouse strain that displays a phenotype of accelerated aging with cognitive decline, as observed in AD, and widely used as a feasible rodent model of cognitive dysfunction [36]. To the best of our knowledge, this manuscript reports the first study including cognitive and behavioral parameters of novel I_2-IR ligands in a well-characterized animal model for studying brain aging and neurodegeneration.

Material and methods

*Synthesis of I_2-IR ligands **MCR5** and **MCR9**.*

The compounds were prepared using our previously optimized conditions [34]. I_2-IR p*K*i for **MCR5** and **MCR9** were determined as 9.42±0.16 nM and 8.85±0.21 nM respectively, showing both compounds also high selectivity *vs.* α_2 adrenergic receptors (457 and 1862, respectively) [35].

The Blood-Brain Barrier (BBB)- determination method

The *in vitro* permeability (Pe) of the novel compounds through a lipid extract of the porcine brain was determined using a mixture of PBS/EtOH 70:30. The concentration of drugs was determined using a UV/VIS (250-500 nm) plate reader. Assay validation was carried out by comparison of the experimental and reported permeability values of 14 commercial drugs (see supporting information), which provided a good linear correlation: Pe (exp) = 1.003 Pe (lit) – 0.783 (R^2 = 0.93). Using this equation and the limits established by Di et al. [37] for BBB permeation, the following ranges of permeability were established: Pe (10^{-6} cm·s^{-1})>5.18 for compounds with high BBB permeation (CNS+); Pe (10^{-6} cm·s^{-1})<2.06 for compounds with low BBB permeation (CNS–); and 5.18>Pe (10^{-6} cm·s^{-1})>2.06 for compounds with uncertain BBB permeation (CNS±).

Measurements of hypothermic effects

For this study, a total of 25 adult male CD-1 mice (30-40 g) bred in the animal facility at the University of the Balearic Islands were used. Mice were housed in standard cages under defined environmental conditions (22°C, 70% humidity, and 12 h light/dark cycle, lights on at 8:00 AM) and with free access to a standard diet and tap water. Experimental procedures followed the ARRIVE [38] and standard ethical guidelines (European Communities Council Directive 86/609/EEC and Guidelines for the Care and Use of Mammals in Neuroscience and Behavioral Research, National Research Council 2003) and were approved by the Local Bioethical Committee (UIB-CAIB). All efforts were made to minimize the number of mice used and their suffering.

Mice were handled, weighted, and habituated to the experimenter for two days before any experimental procedures. For the acute treatment, mice received a single dose of **MCR9** (20mg/kg, i.p., n=6) or vehicle (a mixture of equal parts of DMSO and saline, i.p., n=7), while for the repeated treatment mice were daily treated with **MCR9** (20mg/kg, i.p., n=6) or vehicle (a mixture of equal parts of DMSO and saline, i.p., n=6) for 5 consecutive days. The hypothermic effect of compound **MCR9** was evaluated by measuring rectal temperature before any drug treatment (basal value) and 1h after drug injection by a rectal probe connected to a digital thermometer (Compact LCD thermometer, SA880-1M, RS, Corby, UK). Mice were sacrificed right after the last measurement of rectal temperature.

SAMP8 in vivo experiments

SAMP8 female mice (n=26) (12-month-old) were used to carry out cognitive and molecular analyses. We divided these animals randomly into three groups: SAMP8 Control (SP8-Ct, n=10) and SAMP8 treated with I_2-IR ligands (**MCR5**, n=8) and (**MCR9**, n=8). Animals had free access to food and water and were kept under standard temperature conditions (22±2°C) and 12h: 12h light-dark cycles (300 lux/0 lux). **MCR5** and **MCR9** (5mg/Kg/day) were dissolved in 1,8% 2-hydroxypropyl-β-cyclodextrin and administered through drinking water for 4 weeks. Water consumption was controlled each week, and I_2-IR ligands concentrations were adjusted accordingly to reach the optimal dose.

Studies and procedures involving mice brain dissection and subcellular fractionation were performed by the ARRIVE [38] and international guidelines for the care and use of laboratory animals (see above) and approved by the Ethical Committee for Animal Experimentation at the University of Barcelona.

Open Field (OFT), Elevated Plus Maze (EPM), and Novel Object Recognition Test (NORT)

The OFT apparatus was a white polywood box (50x50x25cm). The floor was divided into two areas defined as center zone and peripheral zone (15cm between the center zone and the wall). Behavior was scored with SMART® ver.3.0 software, and each trial were recorded for later analysis, utilizing a camera situated above the apparatus. 26 mice (n=8-10 per group) were placed at the center and allowed to explore the box for 5 min. Afterward, mice were returned to their home cages, and the OFT apparatus was cleaned with 70% EtOH. The parameters scored included center staying duration, rears, defecations, and the distance traveled, calculated as the sum of total distance traveled in 5 min.

The EMP apparatus consists of opened arms and closed arms, crossed in the middle perpendicularly to each other, and a central platform (5×5cm) constructed of dark and white plywood (30×5×15cm). To initiate the test session, 26 mice (n=8-10 per group) were placed on the central platform, facing an open arm, and allowed to explore the apparatus for 5 min. After the 5 min test, mice were returned to their home cages, and the

EPM apparatus was cleaned with 70% EtOH and allowed to dry between tests. Behavior was scored with SMART® ver.3.0 software, and each trial was recorded for later analysis, utilizing a camera fixed to the ceiling at the height of 2.1m and situated above the apparatus. The parameters recorded included time spent on opened arms, time spent on closed arms, time spent in the center zone, rears, defecation and urination.

The NORT protocol employed was a modification of those of Ennaceur and Delacour [39]. In brief, 26 mice (n=8-10 per group) were placed in a 90°, two-arm, 25-cm-long, 20-cm-high, 5-cm-wide black maze. The walls could be removed for easy cleaning. Light intensity in mid-field was 30 lux. Before performing the test, the mice were individually habituated to the apparatus for 10 min for 3 days. On day 4, the animals were submitted to a 10 min acquisition trial (first trial), during which they were placed in the maze in the presence of two identical, novel objects (A+A or B+B) at the end of each arm. A 10 min retention trial (second trial) was carried out 2h and 24h later, with one of the two objects changed. During these second trials, mice behavior was recorded with a camera. The Time New object (TN) and the Time Old object (TO) were measured. A Discrimination Index (DI) was defined as (TN−TO)/(TN+TO). The maze and the objects were cleaned with 96% EtOH after each test to eliminate olfactory cues.

Brain processing

Mice were euthanized by cervical dislocation one day after the behavioral and cognitive tests finished. Brains were immediately removed from the skull. The hippocampus was then isolated and frozen in powdered dry ice. They were maintained at -80°C for further use. Tissue samples were homogenized in lysis buffer containing phosphatase and protease inhibitors (Cocktail II, Sigma-Aldrich). Total protein levels were obtained and the method of Bradford determined protein concentration.

Protein levels determination by Western blot (WB)

For WB, aliquots of 15μg of hippocampal protein were used. Protein samples from 15 mice (n=5 per group) were separated by SDS-PAGE (8-12%) and transferred onto PVDF membranes (Millipore). Afterward, membranes were blocked in 5% non-fat milk in 0,1% Tween20 TBS (TBS-T) for 1h at room temperature, followed by overnight incubation at 4°C with the primary antibodies listed in Table 1 (Supporting information). Membranes were washed and incubated with secondary antibodies for 1hat room temperature.

Immunoreactive proteins were viewed with a chemiluminescence-based detection kit, following the manufacturer's protocol (ECL Kit; Millipore) and digital images were acquired using a ChemiDoc XRS+ System (BioRad). Semi-quantitative analyses were carried out using ImageLab software (BioRad), and results were expressed in arbitrary units, considering control protein levels as 100%. Protein loading was routinely monitored by immunodetection of glyceraldehyde-3-phosphate dehydrogenase (GAPDH).

Determination of OS in the hippocampus

Hydrogen peroxide (H_2O_2) from 12 mice (n=4 per group) was measured in hippocampal tissue protein extracts obtained as described above, as an indicator of OS and it was quantified using the hydrogen peroxide Assay Kit (Sigma-Aldrich, St. Louis, MI) according to the manufacturer's instructions.

RNA extraction and gene expression determination

Total RNA isolation was carried out using TRIzol® reagent according to manufacturer's instructions. The yield, purity, and quality of RNA were determined spectrophotometrically with a NanoDrop™ ND-1000 (Thermo Scientific) apparatus and an Agilent 2100B Bioanalyzer (Agilent Technologies). RNAs with 260/280 ratios and RIN higher than 1.9 and 7.5, respectively, were selected. Reverse Transcription-Polymerase Chain Reaction (RT-PCR) was performed as follows: 2μg of mRNA was reverse-transcribed using the High Capacity cDNA Reverse Transcription Kit (Applied Biosystems). Real-time quantitative PCR (qPCR) was employed to quantify the mRNA expression of OS genes Heme oxygenase (decycling) 1 (*Hmox1*), Aldehyde oxidase 1 (*Aox1*), Cyclooxygenase 2 (*Cox2*), inflammatory genes Interleukin 6 (*Il-6*), Interleukin 1 beta (*Il-1β*), Tumor necrosis factor alpha (*Tnf-α*), Amyloid processing gene disintegrin and metalloproteinase domain-containing protein 10 (*Adam10*) and amyloid degradation gene Neprilysin (*NEP*). The primers were listed in Table 2 (Supporting information).

SYBR® Green real-time PCR was performed in a Step One Plus Detection System (Applied-Biosystems) employing SYBR® Green PCR Master Mix (Applied-Biosystems). Each reaction mixture contained 7.5μL of cDNA(which concentration was 2μg), 0.75μL of each primer (which concentration was 100nM), and 7.5μL of SYBR® Green PCR Master Mix (2X).

TaqMan-based real-time PCR (Applied Biosystems) was also performed in a Step One Plus Detection System (Applied-Biosystems). Each 20µL of TaqMan reaction contained 9µL of cDNA (25ng), 1µL 20X probe of TaqMan Gene Expression Assays and 10µL of 2X TaqMan Universal PCR Master Mix.

Data were analyzed utilizing the comparative Cycle threshold (Ct) method (ΔΔCt), where the housekeeping gene level was used to normalize differences in sample loading and preparation. Normalization of expression levels was performed with *actin* for SYBR® Green-based real-time PCR results and *Tbp* for TaqMan-based real-time PCR. Each sample (n=4-5 per group) was analyzed in duplicate, and the results represent the n-fold difference of the transcript levels among different groups.

Data analysis

The statistical analysis were conducted using GraphPad Prism ver. 6 statistical software. Data were expressed as the mean ± Standard Error of the Mean (SEM). Means were compared with One-way Analysis of variance (ANOVA) and Tukey's post hoc test or two-tailed Student's *t*-test when it was necessary. Statistical significance was considered when *p* values were <0.05. Statistical outliers were performed out with Grubbs' test and were removed from the analysis.

RESULTS

BBB permeation assay for I_2-IR ligands MCR5 and MCR9

The tested compounds **MCR5** and **MCR9** had Pe values of 13.5±0.9 and 26.9±1.7, respectively, well above the threshold for high BBB permeation, so that they were predicted to be able to cross the BBB and reach their biological target in CNS. Supplementary information on results analysis could be found in supporting material (Table 3).

Hypothermic effects of compound MCR9 in mice

It is known that selective I_2-IR ligands induced hypothermia in rodents [4]. In particular, the hypothermic effect of compound **MCR5** in mice was evaluated in a recent study from our research group (results for compound **2c** in ref 35) [35]. Similar to **MCR5**, the compound **MCR9** induced mild hypothermia as assessed by a moderate reduction (-

2.3°C) in rectal temperature 1h after injection at the tested dose of 20mg/kg in adult CD-1 mice and as compared with vehicle-treated controls (Figure 3A, day 1). While repeated (5 days) administration (20mg/kg) revealed persistent hypothermic effects of **MCR9** from days 1 to 4 (range from -2.3 to -3.2°C), on day 5 no significant effects were observed in body temperature (-1.8°C change) as compared to vehicle-treated controls (Figure 3B).

Beneficial effects on behavior and cognition induced by MCR5 and MCR9 in SAMP8

Results obtained in OFT demonstrated that both compounds were able to increase locomotor activity and time spent in the center zone (Figures 4A and B). Besides, a significant increment in the vertical activity, quantified by the number of total rears, was observed in mice treated with **MCR5** or **MCR9** in OFT and the EPM (Figures 4C and F). EPM data indicated a reduction in anxiety-like behavior by a significant decrease time spent in closed arms for a treated animal compared to control (Figure 4E). These results are supported by a preference for opened arms, although, not significant for **MCR5** (Figure 4D). Moreover, a significant increase in the DI indicates an improved performance in recognition of the new object in the NORT between **MCR5**- and **MCR9**-treated SAMP8 compared to the SAMP8 control group. A robust effect in short (2h) and long-term (24h) memory was found for the two tested compounds (Figures 4G and H).

OS and inflammatory markers reduced by MCR5 and MCR9 in SAMP8

OS and neuroinflammation are thought to be key risk factors in the development of neurodegeneration. The hydrogen peroxide levels in the hippocampus were significantly reduced in brains of treated mice with either **MCR5** or **MCR9** in comparison with the control group (Figure 5A). Of note, superoxide dismutase 1 (SOD1) protein levels were reduced by **MCR5** but not by **MCR9** treated mice (Figure 5B). Moreover, *Hmox1* gene expression, an important key enzyme in cellular antioxidant-defense, was also significantly increased with both candidates, **MCR5** and **MCR9** (Figure 5D). Other OS markers as *Aox1* or *Cox2* were not significantly altered (Figure 5D). Regarding the inflammation markers, no changes were observed in *Il-6* gene expression for tested compounds, but a significant decrease in *Il-1β* and *Tnf-α* for **MCR5** treated SAMP8 was found (Figure 5E). Moreover, a significant diminution in *Gfap* gene expression was determined, reinforcing the prevention of inflammatory processes by **MCR5** and **MCR9** (Figure 5C).

Changes in synaptic markers and apoptotic factors induced by MCR5 and MCR9 in SAMP8

MCR5, but not **MCR9**, induced an increase in Postsynaptic density protein 95 (PSD95) protein levels (Figure 6A). Protein levels for Synaptophysin (SYN), a presynaptic protein, showed a slight increase for both compounds, although did not reach significance (Figure 6B). To determine the implication of proteolytic processes in the **MCR5** and **MCR9** compounds, we found reduced levels of calpain (data not shown) with a significant diminution in 150 α-spectrin breakdown fragment (SPBD) (Figure 6C). Besides, **MCR9** and **MCR5** were able to reduce caspase-3 activity in SAMP8 hippocampi, because of the diminution of caspase-3 protein levels and 120 SPBD fragments that reached significance for **MCR9** (Figure 6C and D). Moreover, B-cell lymphoma 2 (Bcl-2) levels were diminished, and Bcl-2-associated X (Bax), a key protein in the apoptotic cascade, was reduced by **MCR5** (Figures 6E and F), supporting a possible implication of I_2-IR in apoptosis processes.

Changes in Mitogen-activated protein kinases (MAPK) signaling pathways reduced hyperphosphorylation of Tau induced by MCR5 and MCR9 in SAMP8

Key proteins associated with molecular pathways disturbed in brain disorders and neurodegeneration were evaluated by WB. Interestingly, **MCR5**, but not **MCR9**, increased p-AKT/AKT ratio (protein kinase B) (Figure 7A). Accordingly, higher levels of inactivated Glycogen synthase kinase 3 beta (GSK3β), phosphorylated in Ser9, were determined (Figure 7B). Extracellular Signal-regulated Kinase (ERK½) inhibition by **MCR5** and **MCR9** was demonstrated by a reduction of p-ERK½ ratio, (Figure 7C). Furthermore, Cyclin-dependent kinases 5 (CDK5) measured by p-CDK5/CDK5 and p25/p35 ratio were also reduced (Figures 7D and E). Taking into account the results obtained on kinases CDK5, GSK3β, AKT, and ERK½, we studied Tau hyperphosphorylation levels in the hippocampus of SAMP8. A significant reduction in Tau phosphorylation in treated SAMP8 was found, specifically for Ser404 phosphorylation site, whereas Ser396 phosphorylation site was reduced without reaching signification (Figure 7F).

Changes in APP processing and Aβ degradation induced by MCR5 and MCR9 in SAMP8

We found a significant increase in sAPPα protein levels in **MCR9** treated SAMP8 (Figure 8A) and a significant reduction in sAPPβ protein levels in **MCR5** (Figure 8B). Besides, a significant increase in gene expression for *Adam10*, an α-secretase that cleavage APP and *NEP*, an Aβ degrading enzyme (Figures 8C and D) in treated mice groups than in non-treated animals.

DISCUSSION

I_2-IR have been related to several physiological and pathological processes, including CNS ones, such as pain [8], neuropathic pain [40], seizures [41, 42], and neurodegenerative diseases as AD [14, 43]. Our lab has a research line on the development of new high affinity and selectivity I_2-IR ligands, maintaining imidazoline scaffold and incorporating several substituents in the imidazoline ring. Some of them were tested for the neuroprotective role previously [35].

Given the enormous potential of I_2-IR and their implications in brain disorders and neurodegenerative diseases such as AD, we set out to explore whether **MCR5** and **MCR9**, two members of a structurally new family of I_2-IR ligands, might improve the behavioral and cognitive status in the SAMP8 model. Main chemical structural differences were a phosphonate substituent on the imidazoline ring for **MCR5** in contrast with an ester group for **MCR9** (Figure 2).

Published results from our lab demonstrated that **MCR5** presented a p*K*i for the I_2-IR of 9.42±0.16 and high selectivity when compared with α_2 receptors affinity [35]. Likewise, **MCR9** is also a high-affinity I_2-IR ligand (p*K*i 8.85±0.21) but with a higher selectivity against α_2 receptors. Both **MCR5** and **MCR9** were predicted to be able to cross the BBB, a drug characteristic of importance when action is expected in the CNS.

Previous studies have evaluated the effects of selective I_2-IR ligands on inducing hypothermia in rodents [e.g., idazoxan or BU224] [44]. Accordingly, **MCR5** can induce hypothermia in mice, and showed neuroprotective role in kainate-induced seizures, modifying levels of and Fas-associated protein with death domain (FADD) receptor [35]. While acute **MCR5** (5 and 20mg/kg) induced mild hypothermia, repeated (20mg/kg, 5 days) administration of **MCR5** revealed significantly attenuated hypothermic effects from day 2 of treatment, which indicated the induction of tolerance to the hypothermic effects of the drug [35]. For **MCR9** (20mg/kg) repeated (5 days) administration revealed persistent hypothermic effects up to day 4. These results suggest that the slow induction of tolerance to the hypothermic effects caused by **MCR9** might be started following 5 days of drug administration, although a more extended treatment paradigm might be needed for confirmation.

The hypothermic effects exerted by **MCR5** and **MCR9** might be relevant to induce neuroprotection, as it was previously proposed for some of the neuroprotective effects induced by the I_2-IR selective ligand idazoxan. Several experiments have ascertained a possible role for hypothermia in mediating neuroprotection. For example, small drops in temperature exerted neuroprotection in cerebral ischemia [45] and are typically used in the clinic to improve the neurological outcome under various pathological conditions (e.g., stroke, brain injury). Although the mechanisms explaining the neuroprotective effects mediated by hypothermia are not well understood, some researchers suggested that they might be related to the inhibition of glutamate release [46].

SAMP8 has been studied as a non-transgenic murine mouse model of accelerated senescence and late-onset AD. These mice exhibit cognitive and emotional disturbances, probably due to the early development of pathological brain hallmarks, such as OS, inflammation, and activation of neuronal death pathways, which mainly affect cerebral cortex and the hippocampus [47, 48]. To date, this rodent model has not been used to test I_2-IR ligands. Thus, this work is the first investigation about the effects of the improvement of cognitive impairment and behavior in this mice model after treatment with I_2-IR ligands.

Behavioral and cognitive effects were investigated through three well-established tests in SAMP8 the OFT, which is an experiment used to assay general locomotor activity and anxiety in rodents [49]; the EPM, one of the most widely used test for measuring anxiety-like behavior [50] and the NORT, as a standard measure of cognition (short- and long-term memory) [51].

The OFT and EPM parameters indicated a reduction in the cognitive impairment through showing improved locomotor activity jointly with an anti-anxiousness effect. Likewise, the NORT results demonstrated an improvement in cognitive and short and long learning capabilities in hippocampal memory processes. Therefore, all the assessed parameters showed robust beneficial effects on cognition and behavior after **MCR5** and **MCR9** treatment in SAMP8.

Results in cognitive and behavioral effects were supported by a cellular and biochemical assessment of characteristic parameters related to cognitive decline and AD. The compelling evidence demonstrated a neuroprotective role for I_2-IR. The neuroprotective role can be related to OS and inflammation [52], by measuring OS indicators and inflammation markers in SAMP8 brain tissue treated with the I_2-IR ligands, **MCR5** and **MCR9**. Results showed significant reduced hydrogen peroxide levels in hippocampal tissue and increased *Hmox1* gene expression in treated **MCR5** and **MCR9** SAMP8, but not in other sensors for OS as *Aox1* or *Cox2*. SOD1 protein levels were reduced by **MCR5** but not by **MCR9**. Regarding inflammation markers, no changes were observed in *Il-6* gene expression for tested compounds, but a significant decrease in *Il-1β* and *Tnf-α* for **MCR5** treated SAMP8 was found. In addition, reduced astrogliosis was found in treated animals, corroborating a reduced inflammatory environment in hippocampi of **MCR5** and **MCR9** treated SAMP8. Altogether these results showed a relatively weak influence in OS and inflammation mechanisms by I_2-IR ligands in SAMP8 [53-57]. However, a role for those two pathological conditions related to I_2-IR ligands interaction cannot be discarded at all because **MCR5** was able to elicit beneficial effects despite the old age of SAMP8. It is known that aged SAMP8 presented lower inflammation and OS due to being at the endpoint of the senescence process [56, 57]. Therefore it can be challenging to determine drug effects on these processes in aged SAMP8.

MCR5 and **MCR9** effects on key molecular markers for synapsis and apoptosis were studied to unravel the cognitive decline prevention by I_2-IR ligands in SAMP8, which is characterized by alterations in those processes. In consonance with better cognitive performance, the compounds tested increased synaptic markers as SYN and PSD95, indicating a neuroprotective role for **MCR5** and **MCR9**.

There are several cellular and molecular pathways related to a better synaptic performance, including proteolytic and phosphorylation activities or apoptotic processes. Regarding proteolytic processes, calpain is an intracellular protease which cleaves the CDK5 activator p35 to a p25 fragment**. MCR5** and **MCR9** diminished calpain levels and activity with a reduced 150 SPBD fragment. Moreover, a significant p25 protein levels diminution was found in treated SAMP8. A decrease in p25 can also influence CDK5 activity, implicated in Tau phosphorylation [58, 59]. These results indicate that CDK5 phosphorylation activity should be diminished after I_2-IR ligands treatment, corroborating results obtained previously for **MCR5** in a kainate model of neuronal damage [60].

Caspase 3 mediated apoptosis was also addressed. Significant reduction of caspase 3 activity and diminution Bax protein were found in **MCR9** treated SAMP8. Because Bax is described as a pro-apoptotic protein, its diminution indicates a possible protective role for I_2-IR ligands in neurons [61]. By contrast, reduced levels of Bcl-2, considered as an anti-apoptotic protein, deserve further studies; several authors indicate that when Bax is reduced, Bcl-2 is less necessary to block Bax dimer formation to form the mitochondrial pore, activating intrinsic apoptotic pathway, and as consequence cells reduce the Bcl-2 levels as a control mechanism [62].

On the other hand, an increase in p-AKT was induced by the I_2-IR ligands, whereas a decrease in ERK½ activation was observed. p-AKT is able to inactivate by phosphorylation in Ser9, GSK3β a key kinase in the process of Tau hyperphosphorylation and then in the neurofibrillary tangles formation together with CDK5. To this point, **MCR5** and **MCR9** treated SAMP8 showed an increase of Ser9 phosphorylated GSK3β and reduced Tau hyperphosphorylation.

Regarding ERK½ inhibition (reduction of p42/p44) by **MCR5** and **MCR9**, this effect can contribute to beneficial effect elicited by I_2-IR on synaptic markers and Tau phosphorylation processes. ERK½ belongs to a subfamily of MAPKs and plays diverse roles in the CNS as neuronal survival or death, synaptic plasticity, and learning and memory through phosphorylation of regulatory enzymes and kinases, among others [63, 64]. Although crucial for neuronal survival, there is some evidence that prolonged activation of the ERK pathway can induce a deleterious effect to the cell [65, 66]. Interestingly, long-lasting ERK activation in neurons has been demonstrated in neurodegenerative diseases such as AD [67, 68] and PD [69]. Here, the inhibition of this kinase can participate in post-translational modifications in cytoskeletal proteins such as Tau, ameliorating the neuronal network functioning, as demonstrated with a synaptic markers increase.

The relationship among MAPKs, such as ERK½, [70] and PI3K, as AKT, and imidazoline receptors is well defined [71, 72]. In this respect, it has been described that either ERK or AKT can be associated with the multifunctional *Fas*/*FADD* complex [73, 74]. It is known that apoptosis is an important contributor to neurodegeneration [75], and in this regard, FADD protein has been suggested as a putative biomarker for pathological processes associated with the course of clinical dementia [76]. It was described that total FADD has a central role in promoting apoptosis [77, 78] and its phosphorylation at Ser191/194 mediates non-apoptotic actions such as cell growth and differentiation [79]. In previous work, we demonstrated that **MCR5** was able to modify FADD phosphorylation (i.e., increased p-FADD/FADD ratio) in a kainate-treated rat model [35]. These results could explain the modulation of proteins from the apoptotic pathway mentioned before (e.g., a diminution in caspase 3 activation and significant changes in Bcl-2 and Bax), which seems to favor anti-apoptotic actions mediated through I_2-receptors, and especially by **MCR5**.

Tau hyperphosphorylation is one of the histological trends in many neurodegenerative diseases characterized by cognitive decline, including ADtherefore we studied APP processing pathways. Aberrant APP processing is a hallmark of cognitive decline diseases [80]. To assess the capacity of the tested compounds to modify this pathological hallmark, we evaluated APP fragments, concretely sAPPα and sAPPβ. Despite both APP fragments did not reach signification for both I_2-IR ligands treated groups, we found a clear tendency, which indicates the non-amyloidogenic pathway preference. Moreover, sAPPα is described as neuroprotective, neurotrophic and cell excitability and synaptic plasticity regulator [81], *Adam10* [82] and *NEP* [83] gene expression were higher in **MCR5,** and **MCR9** treated mice groups than in non-treated animals. In sum, I_2-IR ligands foster a diminution in the amyloidogenic pathway and higher degradation of β-amyloid in SAMP8 mice model.

In conclusion, the effectiveness of the two new I_2-IR ligands in an *in vivo* female model for cognitive decline, gated to neurodegenerative processes, and AD, as is SAMP8, can open new therapeutic avenues against these pathological conditions with unmet medical needs. Although different authors have previously indicated the relationship between I_2-IR and cognitive decline, this study is the first experimental evidence that demonstrates the possibility to use this receptor as a target for cognitive impairment. Here, we demonstrate that this strategy could be a new challenge in the treatment of these devastating conditions in the future.

Author Contributions

C. G.-F. and F. V. contributed equally. C. G.-F., C. E., L. F. C. and M. P. designed the study. B. P. performed the PAMPA-BBB permeation experiments. C. G.-F. and F. V. carried out the behavior and cognition studies and cellular parameters determination (OS and inflammation markers, synaptic markers and apoptotic factors and hyperphosphorylation of Tau). J. A. G.-S. and M. J. G.-F. performed the hypothermic studies. S. A., S. R.-A. and A. B. synthesized and purified the l_2-IR ligands. C. G.-F., L.

F. C., F. X. S., J. A. G.-S., M. J. G.-F., C. E. and M. P. contributed to writing the manuscript. All authors have read and have approved to the final version of the manuscript.

Acknowledgments

This study was supported by Ministerio de Economía y Competitividad of Spain (SAF2016-33307 and SAF2014-55903-R) and the Basque Government (IT616/13). C. G.-F., F. V., F. X. S., C. E. and M. P. belong to 2017SGR106 (AGAUR, Catalonia). J. A. G.-S. is a member emeritus of the Institut d'Estudis Catalans (Barcelona, Catalonia). Financial support for F.V. (University of Barcelona, APIF_2017), S. R.-A. (Generalitat de Catalunya, 2018FI_B_00227) and A. B. (Institute of Biomedicine UB_2018).

ABBREVIATIONS

AD, Alzheimer's disease; *Adam10,* A Disintegrin and metalloproteinase domain-containing protein 10; ANOVA, One-Way Analysis of Variance; APP, Amyloid precursor protein; *Aox1*, Aldheyde oxidase 1; AKT, protein kinase B; Bcl-2, B-cell lymphoma 2; Bax, Bcl-2-associated X; BBB, Blood-Brain Barrier; CDK5, Cyclin-dependent kinase 5; CNS, central nervous system; *Cox2*, Cyclooxygenase 2; Ct, Cycle threshold; DI, Discrimination Index; EPM, Elevated Plus Maze; ERK, Extracellular signal-regulated kinase; GAPDH, Glyceraldehyde-3-phosphate dehydrogenase; FADD, Fas-Associated protein with Death Domain; *Gfap*, Glial fibrillary acidic protein; GSK3β, Glycogen synthase kinase 3 beta; *Hmox1*, Heme oxigenase (decicling) 1; I_2-IR, I_2-Imidazoline receptors; *Il-1β*, Interleukin 1 beta; *Il-6*, Interleukin 6; MAO,

REFERENCES

1. Bousquet P, Feldman J, Schwarts J. Central cardiovascular effects of alpha-adrenergic drugs: differences between catecholamines and imidazolines. J. Pharmacol. Exp. Ther. 1984;230:232-236.
2. Head GA, Mayorov DN. Imidazoline receptors, novel agents and therapeutic potential. Cardiovasc. Hematol Agents Med. Chem. 2006;4:17-32.
3. Lowry JA, Brown JT. Significance of the imidazoline receptors in toxicology. Clin. Toxicol. 2014;52:454-469.
4. Li, JK. Imidazoline I_2 receptors: An update. Pharmacol. Ther. 2017;178:48-56.
5. Fenton, C, Keating, G M, Lyseng-Williamson KA. Moxonidine: a review of its use in essential hypertension. Drugs 2006;6:477-496.
6. Reid JL. Rilmenidine: A clinical overview. Am. J. Hypertens. 2000;13:106S-111S.

7. Olmos G, Alemany R, Boronat MA, García-Sevilla JA. Pharmacologic and molecular discrimination of I_2-imidazoline receptor subtypes. Ann. N. Y. Acad. Sci. 1999;881:144-160.
8. Li JX, Zhang Y. Imidazoline I2 receptors: target for new analgesics? Eur. J. Pharmacol. 2011;658:49-56.
9. Callado LF, Martín-Gomez JI, Ruiz J, Garibi J, and Meana JJ. Imidazoline I_2 receptors density increases with the malignancy of human gliomas. J. Neurol., Neurosurg. Psychiatry 2004;75:785-787.
10. Regunathan S, Feinstein DL, Reis DJ. Anti-proliferative and anti-inflammatory actions of imidazoline agents. Are imidazoline receptors involved? Ann. N. Y. Acad. Sci. 1999;881:410-419.
11. Ruíz J, Martín I, Callado LF, Meana JJ, Barturen F, García-Sevilla JA. Non-adrenoreceptor [^{3}H] idazoxan binding sites (I_2-imidazoline sites) are increased in postmortem brain from patients with Alzheimer's disease. Neurosci. Lett. 1993;160:109-112.
12. García-Sevilla JA, Escribá PV, Walzer C, Bouras C, Guimón J. Imidazoline receptor proteins in brains of patients with Alzheimer's disease. Neurosci. Lett. 1998;247:95-98.
13. Gargalidis-Moudanos C, Pizzinat N, Javoy-Agid F, Remaury A, Parini A. I_2-imidazoline binding sites and monoamine oxidase activity in human postmortem brain from patients with Parkinson's disease. Neurochem. Int.1997;30:31-36.
14. Meana JJ, Barturen, F, Martín I, García-Sevilla JA. Evidence of increased non-adrenoreceptor [^{3}H]idazoxan binding sites in the frontal cortex of depressed suicide victims. Biol. Psychiatry 1993;34:498-501.
15. García-Sevilla JA, Escribá PV, Sastre, et al. Immunodetection and quantitation of imidazoline receptor proteins in platelets of patients with major depression and in brains of suicide victims. Arch. Gen. Psychiatry 1996;53:803-810.
16. Smith KL, Jessop DS, Finn DP. Modulation of stress by imidazoline binding sites: implications for psychiatric disorders. Stress 2009;12:97-114.
17. Comi E, Lanza M, Ferrari F, Mauri V, Caselli G, Rovati LC. Efficacy of CR4056, a first-in-class imidazoline-2 analgesic drug, in comparison with naproxen in two rat models of osteoarthritis. J. Pain Res. 2017;10:1033-1043.
18. Regunathan S, Reis DJ. Imidazoline receptors and their endogenous ligands. Ann. Rev. Pharmacol. Toxicol. 1996;36:511-544.

19. Dardonville C, Rozas I. Imidazoline binding sites and their ligands: an overview of the different chemical structures. Med. Res. Rev. 2004;24:639-661.

20. Boronat MA, Olmos G, García-Sevilla JA. Attenuation of tolerance to opioid-induced antinociception and protection against morphine-induced decrease of neurofilament proteins by idazoxan and other I_2-imidazoline ligands. Br. J. Pharmacol. 1998;125:175-185.

21. McDonald GR, Olivieri A, Ramsay RR, Holt A. On the formation and nature of the imidazoline I_2 binding site on human monoamine oxidase B. Pharmacol. Res. 2010;62:475-488.

22. Casanovas A, Olmos G, Ribera J, Boronat MA, Esquerda JE, García-Sevilla JA. Induction of reactive astrocytosis and prevention of motoneuron cell death by the I_2-imidazoline receptor ligand LSL 60101. Br. J. Pharmacol. 2000;130:1767-1776.

23. Gustafson I, Westerberg E, Wieloch T. Protection against ischemia-induced neuronal damage by the α_2-adrenoceptor antagonist idazoxan: influence of time of administration and possible mechanisms of action. J. Cereb. Blood Flow Metab. 1990;10:885-894.

24. Qiu WW, Zheng RY. Neuroprotective effects of receptor imidazoline 2 and its endogenous ligand agmatine. Neurosci. Bull. 2006;22:187-191.

25. Gilad GM, Gilad VH. Accelerated functional recovery and neuroprotection by agmatine after spinal cord ischemia in rats. Neurosci. Lett. 2000;296:97-100.

26. Han Z, Xiao MJ, Shao B, Zheng RY, Yang GY, Jin K. Attenuation of ischemia induced rat brain injury by 2-(-2-benzofuranyl)-2-imidazoline, a high selectivity ligand for imidazoline I(2) receptors. Neurol. Res. 2009;31:390-395.

27. Maiese K, Pek L, Berger SB, Reis D J. Reduction in focal cerebral ischemia by agents acting at imidazole receptors. J. Cereb. Blood Flow Metab. 1992;12:53-63.

28. Jiang SX, Zheng RY, Zheng JQ, Li XL, Han Z, Hou ST. Reversible inhibition of intracellular calcium influx through NMDA receptors by imidazoline (I)2 receptor antagonists. Eur. J. Pharmacol. 2010;629:12-19.

29. Ruggiero DA, Regunathan S, Wang H, Milner TA, Reis DJ. Immunocytochemical localization of an imidazoline receptor protein in the central nervous system. Brain Res. 1998;780:270–293.

30. Olmos G, Alemany R, Escriba PV, García-Sevilla JA. The effects of chronic imidazoline drug treatment on glial fibrillary acidic protein concentrations in rat brain. Br. J. Pharmacol. 1994;111:997-1002.
31. Rodríguez-Arellano JJ, Parpura V, Zorec R, Verkhratsky, A. Astrocytes in physiological aging and Alzheimer's disease. Neuroscience 2016;323:170-182.
32. Martín-Gómez JI, Ruíz J, Barrondo S, Callado, LF, Meana JJ. Opposite changes in Imidazoline I_2 receptors and α_2-adrenoceptors density in rat frontal cortex after induced gliosis. Life Sci. 2005;78:205-209.
33. Sica DA. Alpha 1-adrenergic blockers: current usage considerations. J. Clin. Hypertens. (Greenwich) 2005;7:757-762.
34. Abás S, Estarellas C, Luque FJ, Escolano C. Easy access to (2-imidazolin-4-yl)phosphonates by a microwave assisted multicomponent reaction. Tetrahedron 2015;71:2872-2881.
35. Abás S, Erdozain AM, Keller B et al. Neuroprotective effects of a structurally new family of high affinity imidazoline I_2 receptors ligands. ACS Chem. Neurosci. 2017;8:737-742.
36. Morley JE, Farr SA, Kumar VB, Armbrecht HJ. The SAMP8 mouse: a model to develop therapeutic interventions for Alzheimer's disease. Curr. Pharm. Des. 2012;18:1123-1130.
37. Di L, Kerns EH, Fan K, McConnell OJ, Carter G. T. High throughput artificial membrane permeability assay for blood-brain barrier. Eur. J. Med. Chem. 2003;38:223–232.
38. McGrath JC, Lilley E. Implementing guidelines on reporting research using animals (ARRIVE etc.): new requirements for publication in BJP. Br. J. Pharmacol. 2015;172:3189-3193.
39. Ennaceur A, Delacour J. (1988) A new one-trial test for neurobiological studies of memory in rats. 1: Behavioral data. Behav. Brain Res. 1998;31:47-59.
40. Ferrari F, Fiorentino S, Mennuni L, Garofalo P, Letari O, Mandelli S, Giordani A, Lanza M, Caselli G. Analgesic efficacy of CR4056, a novel imidazoline-2 receptor ligand, in rat models of inflammatory and neuropathic pain. 2011;4:111-125.
41. Jackson HC, Ripley TL, Dickinson SL, Nutt DJ. Anticonvulsant activity of the imidazoline 6,7-benzoidazoxan.Epilepsy Res. 1991;9(2):121-126.

42. Min JW, Peng BW, He X, Zhang Y, Li JX. Gender difference in epileptogenic effects of 2-BFI and BU224 in mice. Eur J Pharmacol. 2013;718(1-3):81-86.
43. Keller B, García-Sevilla JA. Immunodetection and subcellular distribution of imidazoline receptor proteins with three antibodies in mouse and human brains: Effects of treatments with I1- and I2-imidazoline drugs. J Psychopharmacol. 2015;29(9):996-1012.
44. Thorn DA, An XF, Zhang Y, Pigini M, Li, JX. Characterization of the hypothermic effects of imidazoline I_2 receptor agonist in rats. Br. J. Pharmacol. 2009;166:1936-1945.
45. Craven JA, Conway EL. Effects of alpha 2-adrenoceptor antagonists and imidazoline 2-receptor ligands on neuronal damage in global ischemia in the rat. Clin. Exp. Pharmacol. Physiol. 1997;24:204-207.
46. Illevich UM, Zornow MH, Choi KT, Scheller M, Strnat MA. Effects of hypothermic metabolic suppression on hippocampal glutamate concentrations after transient global cerebral ischemia. Anesth. Analg. 1994;78:905-911.
47. Takeda T. Senescence-accelerated mouse (SAM) with special references to neurodegeneration models, SAMP8 and SAMP10 mice. Neurochem. Res. 2009;34:639-659.
48. Pallàs M. Senescence-accelerated mice P8: a tool to study brain aging and Alzheimer’s disease in a mouse model. ISRN Cell Biol. 2012:1-12.
49. Archer J. Tests for emotionality in rats and mice: A review. Anim. Behav. 1973;21:205-235.
50. Dawson GR, Tricklebank MD. Use of the elevated plus maze in the search for novel anxiolític agents. Trends Pharmacol. Sci. 1995;16:33-36.
51. Antunes M, Biala G. The novel object recognition memory: neurobiology, test procedure, and its modifications. Cogn. Process. 2012;13:93-110.
52. Gao H-M, Zhou H, Hong JS. Oxidative Stress, Neuroinflammation, and Neurodegeneration. In: Peterson P. K., Toborek M. (Eds) Neuroinflammation and Neurodegeneration, 2014; pp. 81-104, Springer, New York, NY.
53. Fujibayashi Y, Yamamoto S, Waki A, Konishi J, Yonekura Y. Increased mitochondrial DNA deletion in the brain of SAMP8, a mouse model for spontaneous oxidative stress brain. Neurosci. Lett. 1998:254:109-112.

54. Sureda FX, Gutierrez-Cuesta J, Romeu M, Mulero M, Canudas AM, Camins A, Mallol J,Pallàs M. Changes in oxidative stress parameters and neurodegeneration markers in the brain of the senescence-accelerated mice SAMP-8. Exp. Gerontol. 2006;41:360-367.
55. Gutierrez-Cuesta J, Sureda FX, Romeu M, Canudas AM, Caballero B, Coto-Montes A, Camins A, Pallàs M. Chronic administration of melatonin reduces cerebral injury biomarkers in SAMP8. J. Pineal Res. 2007;42:394-402.
56. Griñán-Ferré C, Palomera-Avalos V, Puigoriol-Illamola D, Camins A, Porquet D, Plà V, Aguado F, Pallàs M. Behaviour and cognitive changes correlated with hippocampal neuroinflammaging and neuronal markers in SAMP8, a model of accelerated senescence. Exp. Gerontol. 2016;80:57-69.
57. Griñan-Ferré C, Puigoriol-Illamola D, Palomera-Ávalos, V. et al. Environmental enrichment modified epigenetic mechanisms in SAMP8 mouse hippocampus by reducing oxidative stress and inflammaging and achieving neuroprotection. Front. Aging Neurosci. 2016;8:1-12.
58. Gao L, Tian S, Gao H, Xu Y. Hypoxia increases Abeta-induced tau phosphorylation by calpain and promotes behavioral consequences in AD transgenic mice. J. Mol. Neurosci. 2013;51:138-147.
59. Kimura T, Ishiguro K, Hisanaga S. Physiological and pathological phosphorylation of tau by Cdk5. Front. Mol. Neurosci. 2014;7:1-10.
60. Keller B, García-Sevilla JA. Regulation of hippocampal Fas receptor and death-inducing signaling complex after kainic acid treatment in mice. Prog. Neuropsychopharmacol. Biol. Psychiatry. 2015;3:63:54-62.
61. Cheng EH, Wei MD, Weiler S, Flavell RA. Mak TW, Lindster T, Korsmeyer SJ. BCL-2, BCL-X(L) sequester BH3 domain-only molecules preventing BAX- and BAK-mediated mitochondrial apoptosis. Mol. Cell. 2001;8:705-711.
62. Martin LJ. Mitochondrial and Cell Death Mechanisms in Neurodegenerative Diseases. Pharmaceuticals. 2010;3:839-915.
63. Sweatt JD. The neuronal MAP kinase cascade: a biochemical signal integration system subserving synaptic plasticity and memory. J Neurochem. 2001;76:1–10.
64. Hardingham GE, Bading H. Synaptic versus extransynaptic NMDA receptor signalling: implications for neurodegenerative disorders. Nat. Rev. Neurosci. 2010;11:682-696.

65. Imajo M, Tsuchiya Y, Nishida E. Regulatory mechanisms and functions of MAP Kinase signalling pathways. IUBMB Life 2006;58:312-317.
66. Cruz. CD, Cruz F. The ERK 1 and 2 pathway in the nervous system: from basic aspects to possible clinical applications in pain and visceral dysfunction. Curr. Neuropharmacol. 2007;5:244-252.
67. Hyman BT, Elvhage TE, Reiter J. Extracellular signal regulated kinases. Localization of protein and mRNA in the human hippocampal formation in Alzheimer's disease. Am. J. Pathol. 1994;144:565-572.
68. Russo C, Dolcini V, Salis S, Venezia V, Zambrano N, Russo, T, Schettini G. Signal transduction through tyrosine-phosphorylated C-terminal fragments of amyloid precursor protein via an enhanced interaction with Shc/Grb2 adaptor proteins in reactive astrocytes of Alzheimer's disease brain. J. Biol. Chem. 2002; 277: 35282-35288.
69. Kulich SM, Chu, CT. Sustained extracellular signal-regulated kinase activation by 6-hydroxydopamine: implications for Parkinson's disease. J. Neurochem. 2001;77:1058-1066.
70. Montolio M, Gregori-Puigjané E, Pineda D, Mestres J, Navarro P. Identification of small molecule inhibitors of amyloid β-induced neuronal apoptosis acting through the imidazoline I(2) receptor. J. Med. Chem. 2012;55(22):9838-46.
71. Zhang F, Ding T, Yu L, Zhong Y, Dai H, Yan M. Dexmedetomidine protects against oxygen-glucose deprivation-induced injury through the I2 imidazoline receptor-PI3K/AKT pathway in rat C6 glioma cells. J Pharm Pharmacol. 2012;64(1):120-7.
72. Xuanfei L, Hao C, Zhujun Y, Yanming L, Jianping. Imidazoline I2 receptor inhibitor idazoxan regulates the progression of hepatic fibrosis via Akt-Nrf2-Smad2/3 signaling pathway. Oncotarget. 2017;8(13):21015-21030.
73. García-Fuster, MJ, Miralles, A, and García-Sevilla, JA. Effects of opiate drugs on Fas-Associated Protein with Death Domain (FADD) and effector caspases in the rat brain: Regulation by the ERK1/2 MAP kinase pathway. Neuropsychopharmacology 2007;32:399-411.
74. Ramos-Miguel A, García-Fuster MJ, Callado LF, La Harpe R, Meana JJ, García-Sevilla JA. Phosphorylation of FADD (Fas-associated death domain protein) at serine 194 is increased in the prefrontal cortex of opiate abusers: relation to mitogen activated protein kinase, phosphoprotein enriched in astrocytes of 15 kDa,

and Akt signaling pathways involved in neuroplasticity. Neuroscience 2009;161:23-38.

75. Papaliagkas V, Anogianaki A, Anogianakis G, Ilonidis G. The proteins and the mechanisms of apoptosis: A mini-review of the fundamentals. Hippokratia 2007;11:108-113.
76. Ramos-Miguel A, García-Sevilla JA, Barr A. et al. Decreased cortical FADD protein is associated with clinical dementia and cognitive decline in an elderly community sample. Mol. Neurodegener. 2017;12:26.
77. Chinnaiyan AM, O'Rourke K, Tewari M, Dixit VM. FADD, a novel death domain-containing protein, interacts with the death domain Fas and initiates apoptosis. Cell. 1997;81:505-512.
78. Scott FL, Stec B, Pop C, et al. The Fas-FADD death domain complex structure unravels signalling by receptor clustering. Nature 2009; 457:1019-1022.
79. Alappat EC, Feig C, Boyerinas B. et al. Phosphorylation of FADD at serine 194 by CKIα regulates its nonapoptotic activities. Mol. Cell. 2005;19:321-332.
80. O'Brien RJ, Wong PC. Amyloid precursor protein processing and Alzheimer's disease. Annu. Rev. Neurosci. 2011;34:185-204.
81. Gralle M, Botelho MG, Wouters FS. Neuroprotective secreted amyloid precursor protein acts by disrupting amyloid precursor protein dimers. J. Biol. Chem. 2016; 284:15016-15025.
82. Lichtenthaler SF. Alpha-secretase cleavage of the amyloid precursor protein: proteolysis regulated by signaling pathways and protein trafficking. Curr. Alzheimer Res. 2012;9:165-177.
83. El-Amouri SS, Zhu H, Yu J, Marr R, Verma IM, Kindy MS. Neprilysin: An Enzyme Candidate to Slow the Progression of Alzheimer's Disease. Am. J. Pathol.2008;172:1342-1354.

Figure 1. Representative I_2-IR ligands.

Figure 2. Structure of I_2-IR ligands **MCR5** and **MCR9**.

Figure 3. Acute and repeated measurement of the hypothermic effect of compound **MCR9** in mice. (A) Effect of acute treatment with **MCR9** (20mg/kg, i.p.) on rectal body temperature in mice. Columns are means ± SEM of the difference (Δ, 1h - basal value) in body temperature (°C) for **MCR9**-treated mice compared to vehicle-treated **Control** mice. Data were analyzed using Student t-test. ***p*<0.01. (B) Effect of repeated (5 days) treatments with **MCR9** (20mg/kg, i.p., closed circles) on rectal body temperature in mice. Circles are means ± SEM of the difference (Δ, 1h - basal value) in body temperature (°C) for **MCR9**-treated mice compared to vehicle-treated **Controls**. Data were analyzed by using repeated measures ANOVA followed by Sidak's multiple comparison test. ***p*<0.01, ****p*<0.001; (n=6-7 animals per group).

Figure 4. Behavioral and cognitive improvement in SAMP8 12-month-old treated mice with both I_2-IR ligands. (A) A significant increase in the distance travelled in the open field test in I_2-IR ligands treated groups in comparison with the **Control** group. (B) A significant increase in the percentage of time in the center zone of the opened field test in **MCR5** treated group compared to the **Control** group, and no significant difference between **MCR9** and the **Control** group. (C) A significant increase in the number of total rears of the opened field test among groups. (D) The time spent in the opened arms of the EPM did not differ among groups. (E) A significant increase in the time spent in the closed arms among **Control** group in comparison with treated groups. (F) A significant increase in the number of total rears of the EPM in **MCR5** group in comparison with **Control** group. (G) The results of the NORT in the short-term memory 2h revealed a significant increase in both I_2-IR ligands treated groups in comparison with the **Control** group as well as a significant reduction in the DI of **MCR9** group compared to **MCR5** group, and (H) a significant increase in the DI of the long-term memory 24h in both I_2-IR ligands treated groups compared to the **Control** group. Data expressed as means ± SEM (n=8-10 animals per group) and analyzed using a One-way ANOVA followed by Tukey's post hoc test for multiple comparisons. **p*<0.05, ***p*<0.01, ****p*<0.001 and *****p*<0.0001.

Figure 5. Reduced OS and inflammatory markers in SAMP8 12-month-old treated mice with both I_2-IR ligands. (A) There was a significant reduction in hydrogen peroxide concentration in both I_2-IR ligands treated groups in comparison with the **Control** group in homogenates of the hippocampus tissue**.** (B) A significant reduction in protein levels

of SOD1 in **MCR5** group compared to the **Control** group and no difference between **MCR9** and **Control** group. (C) A significant reduction in protein levels of *Gfap* in **MCR5** and **MCR9** in comparison with the **Control** group. (D) Gene expression of antioxidant enzymes in the mice hippocampus. A significant increase in *Hmox1* gene expression, but not for *Aox1* and *Cox2*, among both I_2-IR ligands and **Control** group. (E) Significant reduction in gene expression of *Il-1β and Tnf-α* in **MCR5** group in comparison with the **Control** group, and a tendency to reduce in **MCR9** group for the same genes. However, *Il-6* gene expression did not differ among groups. Values in bar graphs are adjusted to 100% for protein level of the **Control** group. Gene expression levels were determined by real-time PCR. Data expressed as means ± SEM (n=4-5 animals per group) and analyzed using a One-way ANOVA followed by Tukey's post hoc test for multiple comparisons. *p<0.05.

Figure 6. Changes in synaptic markers and apoptotic factors in 12-month-old treated SAMP8 mice with both I_2-IR ligands. (A) A significant increase in protein levels of PSD95 in **MCR5** group in comparison with the other two groups. (B) A tendency to increase in protein levels of SYN in both I_2-IR ligands treated groups in comparison with the **Control** group. (C) There was a tendency to reduce in the spectrin fragment SPBD 150, and a significant reduction in the spectrin fragment SPBD 120 in **MCR9** group in comparison with the **Control** group. (D) A significant reduction in Caspase-3 protein levels in both I_2-IR ligands group in comparison with the **Control** group. (E) A significant reduction in Bcl-2 protein levels in both I_2-IR ligands group in comparison with the **Control** group. (F) A significant reduction in Bax protein levels among the **MCR9** group and the other groups. Values in bar graphs are adjusted to 100% for protein level of the **Control** group. Representative WB for each protein in the hippocampus mice was showed. Data expressed as means ± SEM (n=5 animals per group) and analyzed using a One-way ANOVA followed by Tukey's post hoc test for multiple comparisons. *p<0.05, **p<0.001.

Figure 7. Changes in kinases signaling pathways reduced hyperphosphorylation of Tau in 12-month-old SAMP8 treated with both I_2-IR ligands. (A) Significant increase in the p-AKT ratio in the **MCR5** group in comparison with the others two groups. (B) Significant increase of inactive p-GSK3β (Ser9) protein levels in both I_2-IR ligands

treated groups compared to the **Control** group. (C) Significant reduction in p-ERK½ in both I_2-IR ligands treated groups in comparison with the **Control** group. (D) Changes in p-CDK5/CDK5 ratio induced by **MCR5** and **MCR9** treatment. (E) Changes in p25/p35 ratio in the **MCR5** and **MCR9** group in comparison with the **Control group**. Representative WB were showed. (F) A reduction in p-Tau (Ser396), as well as a significant reduction in p-tau (Ser404) in both I_2-IR ligands treated groups in comparison with the **Control** group. Values in bar graphs were adjusted to 100% for protein level of the **Control** group. Data expressed as means ± SEM (n=5 animals per group) and analyzed using a One-way ANOVA followed by Tukey's post hoc test for multiple comparisons. *p<0.05, **p<0.01, ***p<0.001.

Figure 8. Changes in APP processing and Aβ degradation enzymes in SAMP8 12-month-old treated with both I_2-IR ligands. Representative WB of the APP, and its fragments. (A) Significant increase in sAPPα protein levels in **MCR9** group compared to the **Control** group, and no significant difference between **MCR5** and the **Control** group. (B) Significant reduction in sAPPβ in protein levels in **MCR5** group compared to the **Control** group, and no significant difference between **MCR9** and the **Control** group. (C) Significant increase in gene expression of *Adam10* in **MCR5** group compared to the **Control** group, and no significant difference in **MCR9** group. (D) There was a significant increase in gene expression of *NEP* in **MCR5** group compared to the **Control** group, and no significant difference in **MCR9** group. Values in bar graphs were adjusted to 100% for protein level of the **Control** group. Gene expression levels were determined by real-time PCR. Data expressed as means ± SEM (n=4-5 animals per group) and analysed using a One-way ANOVA followed by Tukey's post hoc test for multiple comparisons. *p<0.05.

Figure 1

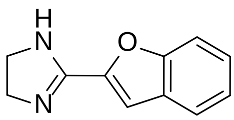

2-BFI

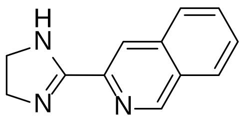

BU-224

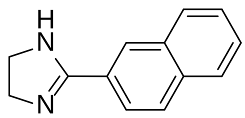

benazoline

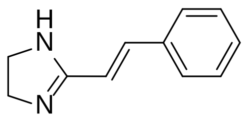

valldemossine (tracizoline)

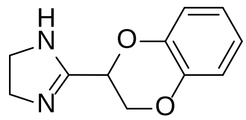

idazoxan

Figure 2

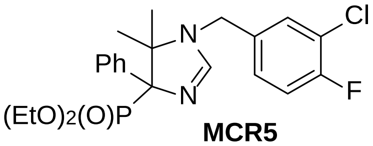

MCR5

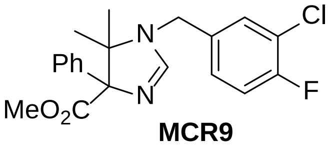

MCR9

Figure 3

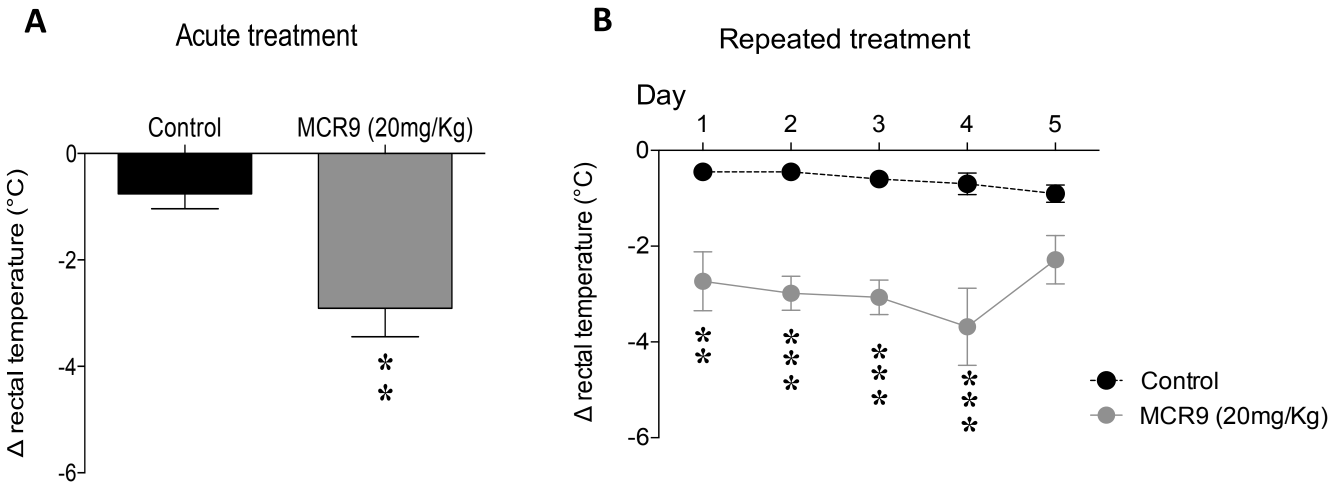

A
Acute treatment
Control
MCR9 (20mg/Kg)
0
-2
-4
-6
Δ rectal temperature (°C)
**
B
Repeated treatment
Day
1
2
3
4
5
0
-2
-4
-6
Δ rectal temperature (°C)
**
***
***
***
Control
MCR9 (20mg/Kg)

Figure 4

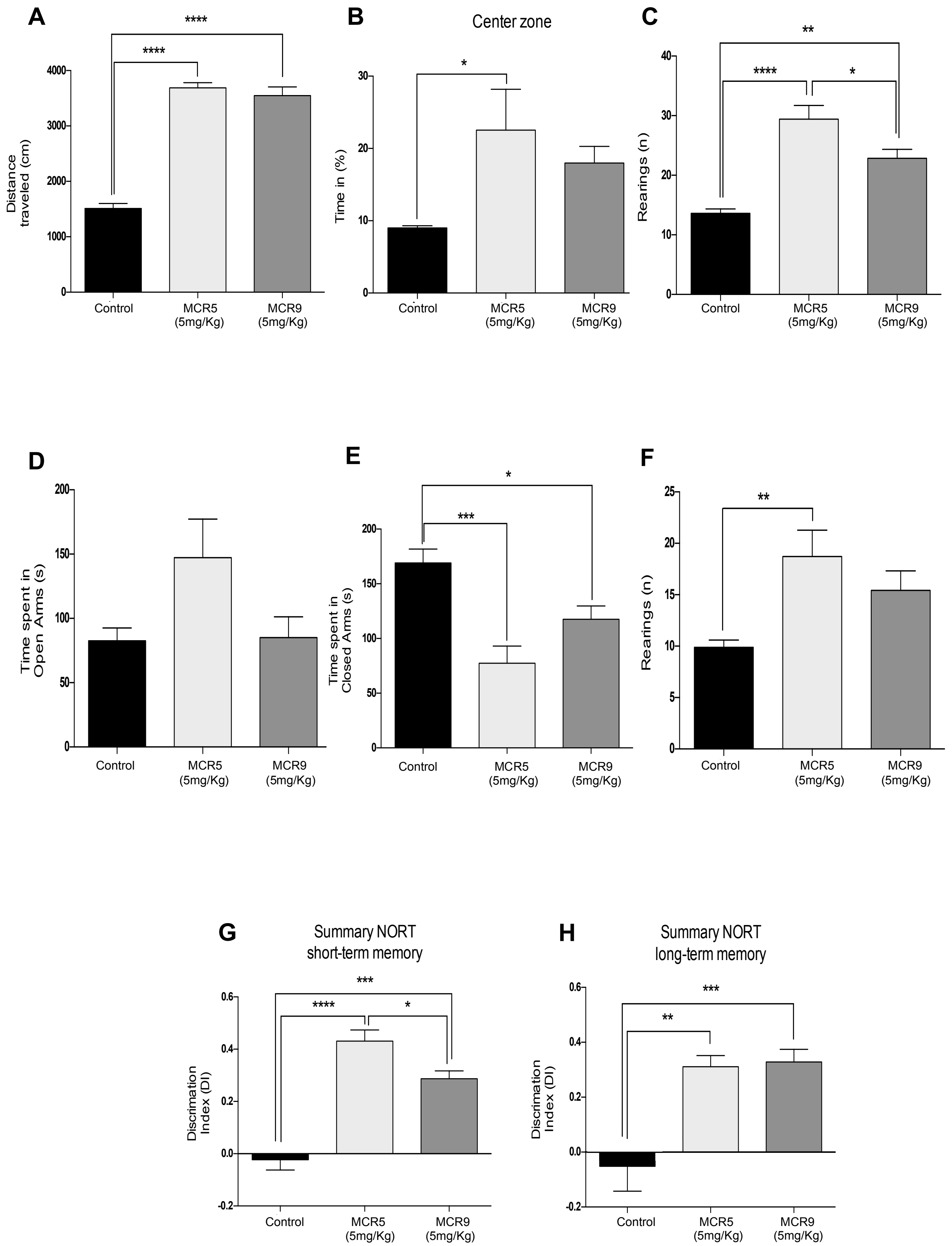

A
Distance traveled (cm)
Control
MCR5 (5mg/Kg)
MCR9 (5mg/Kg)
B
Center zone
Time in (%)
C
Rearings (n)
D
Time spent in Open Arms (s)
E
Time spent in Closed Arms (s)
F
Rearings (n)
G
Summary NORT short-term memory
Discrimation Index (DI)
H
Summary NORT long-term memory

Figure 5

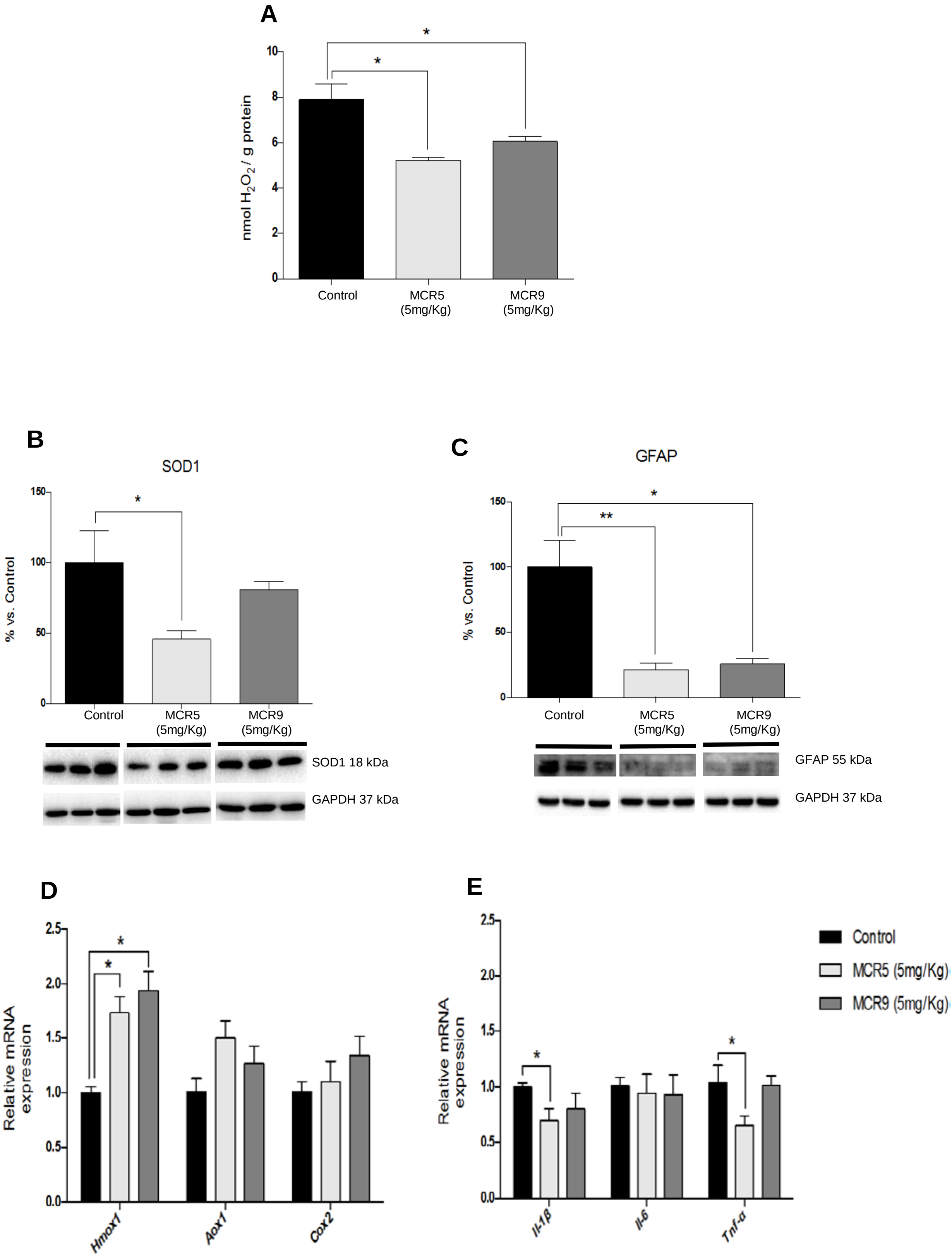
A
nmol H2O2 / g protein
Control
MCR5 (5mg/Kg)
MCR9 (5mg/Kg)
B
SOD1
% vs. Control
SOD1 18 kDa
GAPDH 37 kDa
C
GFAP
GFAP 55 kDa
GAPDH 37 kDa
D
Relative mRNA expression
Hmox1
Aox1
Cox2
E
Il-1β
Il-6
Tnf-α
Control
MCR5 (5mg/Kg)
MCR9 (5mg/Kg)

Figure 6

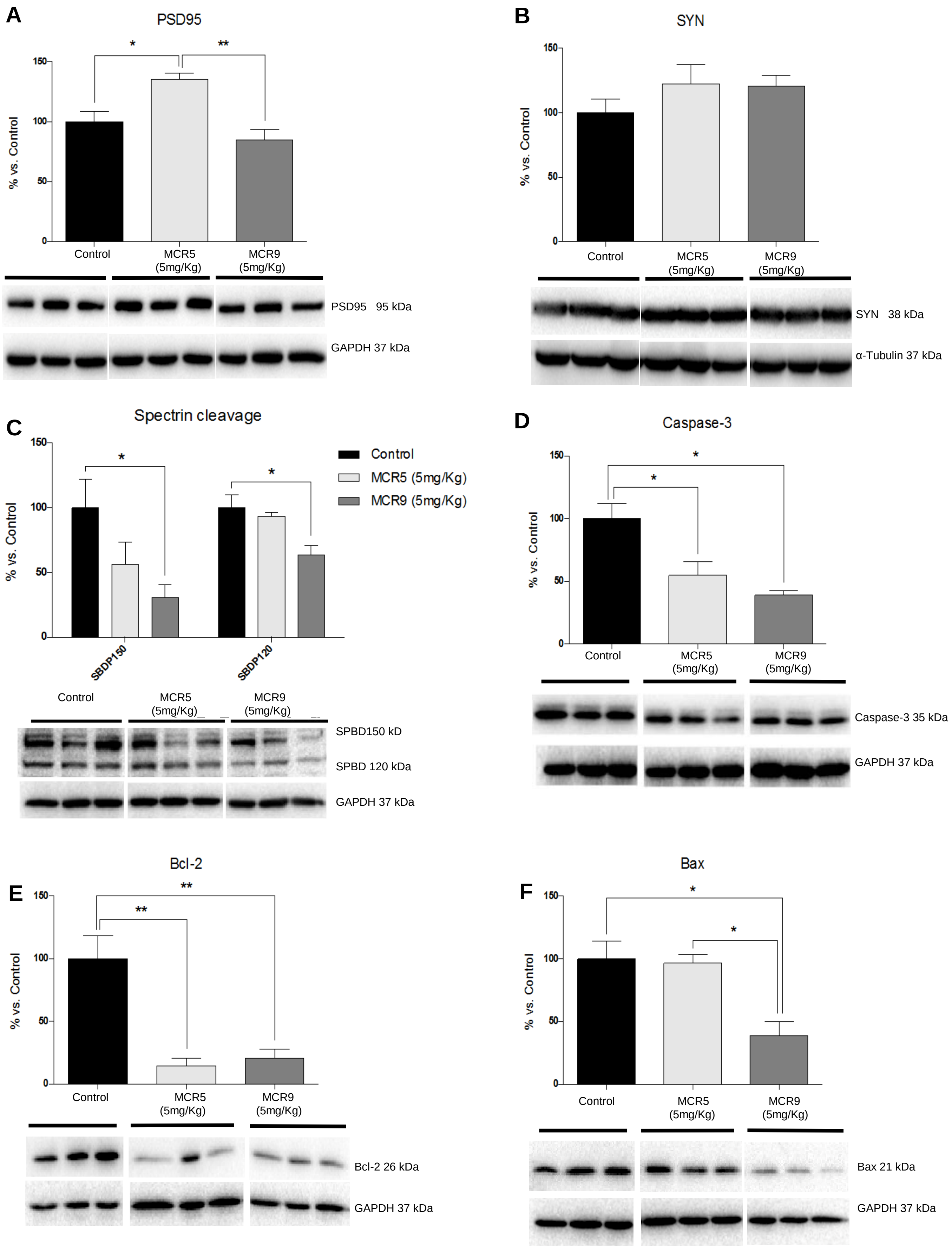

A
PSD95
*
**
% vs. Control
Control
MCR5 (5mg/Kg)
MCR9 (5mg/Kg)
PSD95 95 kDa
GAPDH 37 kDa
B
SYN
% vs. Control
Control
MCR5 (5mg/Kg)
MCR9 (5mg/Kg)
SYN 38 kDa
α-Tubulin 37 kDa
C
Spectrin cleavage
Control
MCR5 (5mg/Kg)
MCR9 (5mg/Kg)
% vs. Control
SBDP150
SBDP120
SPBD150 kD
SPBD 120 kDa
GAPDH 37 kDa
D
Caspase-3
% vs. Control
Caspase-3 35 kDa
GAPDH 37 kDa
E
Bcl-2
% vs. Control
Bcl-2 26 kDa
GAPDH 37 kDa
F
Bax
% vs. Control
Bax 21 kDa
GAPDH 37 kDa

Figure 7

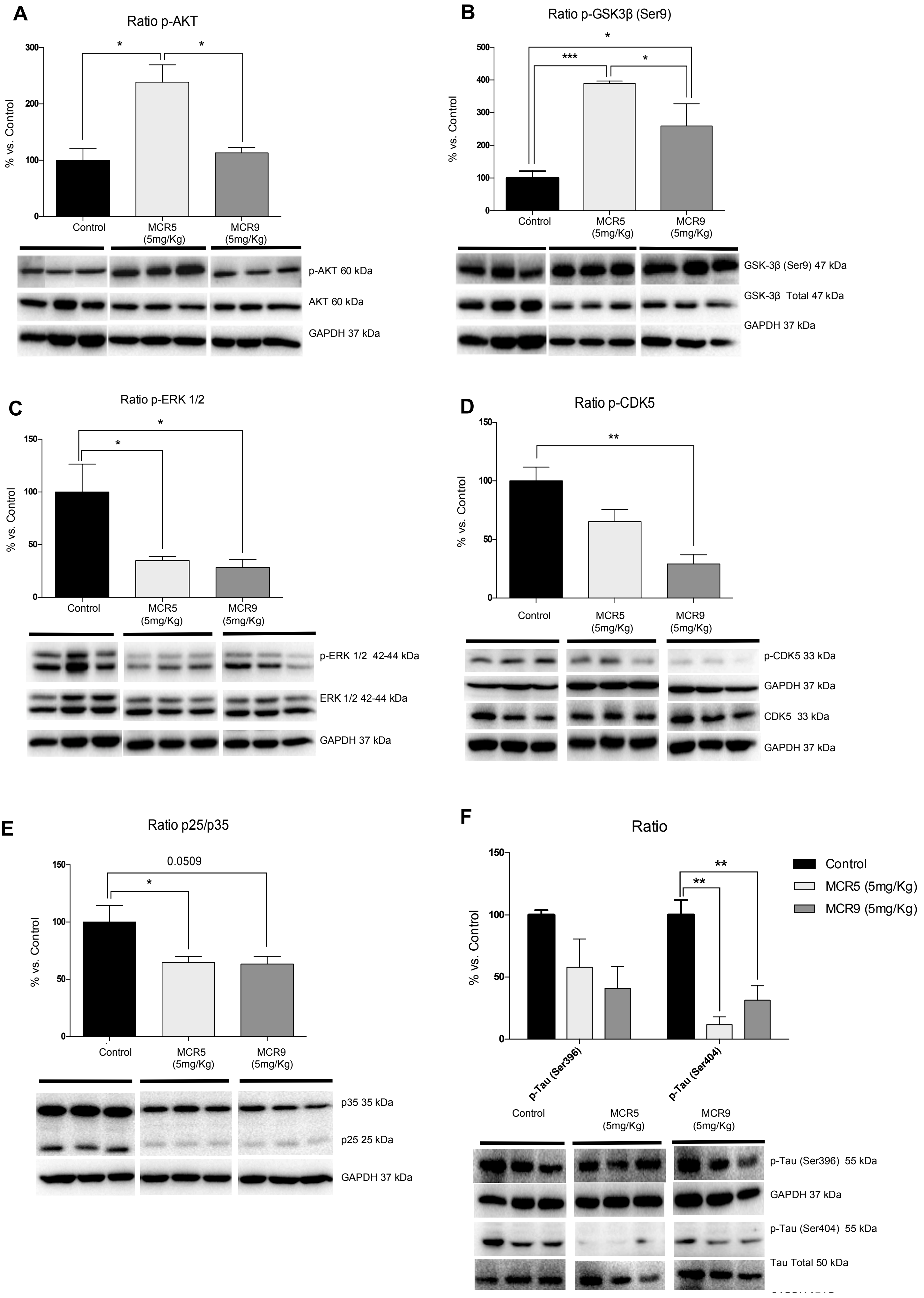

A
Ratio p-AKT
% vs. Control
0
100
200
300
*
*
Control
MCR5 (5mg/Kg)
MCR9 (5mg/Kg)
p-AKT 60 kDa
AKT 60 kDa
GAPDH 37 kDa
B
Ratio p-GSK3β (Ser9)
% vs. Control
0
100
200
300
400
500
*
***
*
Control
MCR5 (5mg/Kg)
MCR9 (5mg/Kg)
GSK-3β (Ser9) 47 kDa
GSK-3β Total 47 kDa
GAPDH 37 kDa
C
Ratio p-ERK 1/2
% vs. Control
0
50
100
150
*
*
Control
MCR5 (5mg/Kg)
MCR9 (5mg/Kg)
p-ERK 1/2 42-44 kDa
ERK 1/2 42-44 kDa
GAPDH 37 kDa
D
Ratio p-CDK5
% vs. Control
0
50
100
150
**
Control
MCR5 (5mg/Kg)
MCR9 (5mg/Kg)
p-CDK5 33 kDa
GAPDH 37 kDa
CDK5 33 kDa
GAPDH 37 kDa
E
Ratio p25/p35
% vs. Control
0
50
100
150
0.0509
*
Control
MCR5 (5mg/Kg)
MCR9 (5mg/Kg)
p35 35 kDa
p25 25 kDa
GAPDH 37 kDa
F
Ratio
% vs. Control
0
50
100
150
**
**
Control
MCR5 (5mg/Kg)
MCR9 (5mg/Kg)
p-Tau (Ser396)
p-Tau (Ser404)
Control
MCR5 (5mg/Kg)
MCR9 (5mg/Kg)
p-Tau (Ser396) 55 kDa
GAPDH 37 kDa
p-Tau (Ser404) 55 kDa
Tau Total 50 kDa

Figure 8

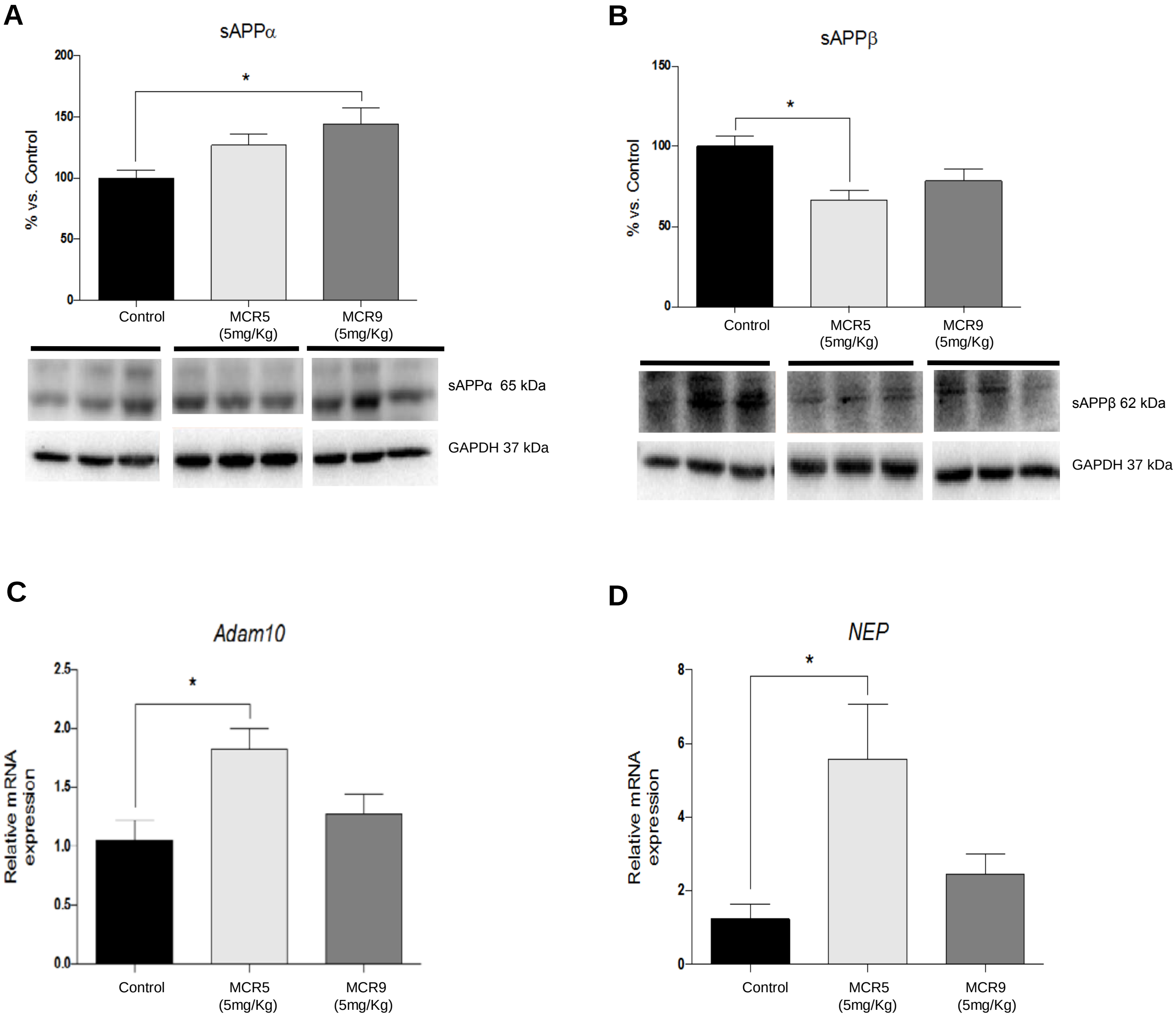
A
sAPPα
% vs. Control
200
150
100
50
0
*
Control
MCR5 (5mg/Kg)
MCR9 (5mg/Kg)
sAPPα 65 kDa
GAPDH 37 kDa
B
sAPPβ
% vs. Control
150
100
50
0
*
Control
MCR5 (5mg/Kg)
MCR9 (5mg/Kg)
sAPPβ 62 kDa
GAPDH 37 kDa
C
Adam10
Relative mRNA expression
2.5
2.0
1.5
1.0
0.5
0.0
*
Control
MCR5 (5mg/Kg)
MCR9 (5mg/Kg)
D
NEP
Relative mRNA expression
8
6
4
2
0
*
Control
MCR5 (5mg/Kg)
MCR9 (5mg/Kg)

Click here to access/download
Conflict of Interest Form
Conflict of Interest Form.pdf

Click here to access/download
Conflict of Interest Form
Conflict of Interest FormAB.pdf

Click here to access/download
Conflict of Interest Form
Conflict of Interest FormBP.pdf

Click here to access/download
Conflict of Interest Form
Conflict of Interest FormCE.pdf

Click here to access/download
Conflict of Interest Form
Conflict of Interest FormCGF.pdf

Click here to access/download
Conflict of Interest Form
Conflict of Interest FormFV.pdf

Click here to access/download
Conflict of Interest Form
Conflict of Interest FormFXS.pdf

Click here to access/download

Conflict of Interest Form

Conflict of Interest FormJAGS.pdf

Click here to access/download
Conflict of Interest Form
Conflict of Interest FormLFCP.pdf

Click here to access/download
Conflict of Interest Form
Conflict of Interest FormMJGF.pdf

Click here to access/download
Conflict of Interest Form
Conflict of Interest FormSA.pdf

Click here to access/download

Conflict of Interest Form

Conflict of Interest FormSRA.pdf